CAMBRIDGE UNIVERSITY PRESS

Tulaneia amabilia n. gen. n. sp.: a new erniettomorph from the Wood Canyon Formation, Nevada and the age of the Ediacaran–Cambrian transition in the Great Basin

Bruce Runnegar[1] , Robert J. Horodyski[2], James G. Gehling[3], Sören Jensen[4], Stefan Bengtson[5], Kevin J. Peterson[6], Matthew R. Saltzman[7] and Michael J. Vendrasco[8]

[1]Department of Earth, Planetary and Space Sciences and Molecular Biology Institute, University of California, Los Angeles, CA 90095-1567, USA
[2]Deceased; formerly, Geology Department, Tulane University, New Orleans, LA 70118-5698, USA
[3]Palaeontology Division, South Australian Museum, Adelaide, South Australia 5000, Australia
[4]Área de Paleontología, Facultad de Ciencias, Universidad de Extremadura, E-06006, Badajoz, Spain
[5]Deceased; formerly, Department of Palaeozoology, Swedish Museum of Natural History, 114 18 Stockholm, Sweden
[6]Department of Biological Sciences, Dartmouth College, Hanover, NH 03755, USA
[7]School of Earth Sciences, Ohio State University, Columbus, OH 43210, USA
[8]Department of Geology, Pasadena City College, Pasadena, CA 91106, USA

Abstract

Specimens of *Tulaneia amabilia* Runnegar and Horodyski n. gen n. sp. (previously *Ernietta plateauensis* Pflug) discovered by RJH in 1991 at a site in the Montgomery Mountains near Johnnie, Nevada, are described for the first time. All of the material from the original locality was from float, but its stratigraphic position within the lowest siliciclastic to dolostone interval of the lower member of the Wood Canyon Formation (LMWCF) was confirmed by subsequent discoveries. Because the upper part of the LMWCF contains *Treptichnus pedum* (Seilacher), the Ediacaran–Cambrian boundary has long been drawn at its first appearance. However, in the Esmeralda Member of the Deep Spring Formation in the White-Inyo Mountains, California, and at Mount Dunfee, Nevada, another Cambrian ichnofossil, '*Plagiogmus*', which is now *Psammichnites gigas arcuatus* (Roedel), is found just beneath the nadir of the basal Cambrian isotope excursion (BACE). Because the nadir of the BACE excursion is older than ca. 539 Ma in Mexico, the oldest occurrences of *Treptichnus pedum* in the LMWCF are latest—not earliest—Fortunian in age, and there is no need to reduce the age of the eon boundary from ca. 539 to ca. 533 Ma. *Tulaneia* resembles *Ernietta* and other erniettomorphs in being composed of tubular modules with planar common surfaces, but its overall shape was tabular and unidirectional rather than sack or frond shaped. We also illustrate and briefly describe other trace and body fossils from the LMWCF and re-illustrate previously published specimens of *Psammichnites gigas arcuatus* in order to document its earliest occurrence in the Great Basin.

UUID: http://zoobank.org/117efe63-c3b8-4c42-8a27-83af05630f48

Non-technical Summary

This work describes and illustrates Ediacaran (latest Precambrian) and Cambrian body and trace fossils from Nevada and California and discusses their significance for understanding the early evolution of animals and for locating the Ediacaran–Cambrian boundary (about 539 million years ago) in sedimentary deposits of the southwestern Great Basin. The most distinctive body fossil is a new air-bed-like organism formed of tubular modules arranged lengthwise. At the growing ends, the tubular modules separated from each other and tapered to blunt points. How these organisms lived and functioned remain uncertain, partly because the fossils are found in deep water deposits far from where they lived. We also deal with another distinctive fossil, '*Plagiogmus*', which was found during the 1960s, but largely ignored or misinterpreted since then. '*Plagiogmus*' is the complex, often meandering burrow of a sizeable slug-like animal that first appeared in earliest Cambrian time. Its association in time with an important geochemical event suggests that the Ediacaran–Cambrian boundary in the Great Basin is older than previously thought.

Introduction

This work describes and illustrates Ediacaran (latest Precambrian) and Cambrian body and trace fossils from Nevada and California and discusses their significance for understanding the early evolution of animals and for locating the Ediacaran–Cambrian boundary in sedimentary deposits of the southwestern Great Basin. We first recount the discovery of Ediacaran body fossils in the craton margin succession of the Death Valley area, and then briefly discuss previous biostratigraphic work on the Precambrian–Cambrian boundary in both the Death Valley and White Inyo regions of California and Nevada and (Figs. 1–4). In following sections, we describe and illustrate the fossils (Figs. 4–12), summarize the results of this investigation, and conclude with a brief discussion of the significance of this work for Ediacaran paleobiology and the age of the eon boundary.

Bob Horodyski (RJH) was prospecting for Precambrian fossils in the craton margin succession of the Death Valley area when he investigated the northern end of the Montgomery Mountains, near the derelict mining town of Johnnie, Nevada, early in 1991. He found a slab of sandstone (Fig. 5.2, B), which had two spectacular fossils—one on each side—that were novel to the succession and clearly not of Cambrian age. After returning to Tulane University, where he photographed the slab, he sent prints to BR and asked for advice as he was planning to submit an abstract for the annual meeting of Geological Society of America (GSA) in San Diego, California. BR enthusiastically (but erroneously) identified the fossils as *Ernietta* Pflug (1966) in a fax sent to RJH on June 24, 1991, and drew his attention to Richard Jenkins' re-analysis of Pflug's (1972) material (Jenkins et al., 1981). The abstract was submitted and published (Horodyski, 1991) and the discovery specimens and others collected during the summer of 1991 were displayed at a poster session in San Diego in October (McMenamin, 1998, p. 30). The discovery slab had obviously not moved far from outcrop, so RJH began a systematic search of the site that took several days. He painstakingly examined each and every loose piece of rock in the vicinity of his discovery and built cairns (Fig. 4.3) from the pieces that lacked fossils. By August 1991, he had assembled the small collection of internal molds (parts) and external molds (counterparts) that now become the holotype and paratypes of the new genus and species *Tulaneia amabilia* Runnegar and Horodyski (Figs. 5–8).

In the GSA abstract, the stratigraphic setting of RJH's discovery was described as "near the contact of the Wood Canyon Formation and the Stirling Quartzite" (Horodyski, 1991, p. A163). Subsequent fieldwork allowed RJH to source the float specimens to the lowest 10–15 m of the Wood Canyon Formation, to measure a stratigraphic section along an adjacent ridge (Figs. 1.2, 4.1), and to find Cambrian trace fossils, including unquestionable specimens of *Treptichnus pedum* (Seilacher, 1955), in the upper part of the lower member of the Wood Canyon Formation (LMWCF; Fig. 10.2, Supplemental dataset 1). Follow-up fieldwork by RJH and the other authors in January and March–April 1993 and March 1995 gave rise to two other GSA abstracts (Horodyski et al., 1994; Runnegar, 1998), but publication of the evidence for these statements is long overdue. This article attempts to remedy that situation.

Geological setting

Lithostratigraphy and geochronology. The stratigraphic nomenclature for the Proterozoic–Cambrian succession of the Death Valley region established by Stewart (1966, 1970) has persisted with little change (Prave et al., 1991; Smith et al., 2023). The sections of interest lie between the top of the Stirling Quartzite and the regional unconformity at the base of the middle member of the Wood Canyon Formation near Johnnie in the Montgomery Mountains, Nye County, Nevada; at Chicago Pass in the Nopah Range, Inyo County, California; south of Wood Canyon in the Spring Mountains, Nye County, Nevada; and in the central Desert Range, Desert National Wildlife Range, Clark County, Nevada (Figs. 1.1, 1.2, 2–4, Appendix 1).

The Stirling Quartzite and the middle member of the Wood Canyon Formation were both deposited during sea level lowstands in shoreface and fluvial environments whereas the intervening LMWCF was formed in deeper marine environments that accumulated micaceous siltstones, hummocky cross-stratified sandstones, and subtidal to peritidal dolostones (Diehl, 1976; Fedo and Cooper, 1990, 2001; Muhlbauer et al., 2020; Nelson et al., 2023). The sequence stratigraphy of the 'Death Valley facies' (Nelson, 1978) has been extensively investigated and there is consensus that the disconformity at the base of the middle member of the Wood canyon Formation is the base of the Sauk megasequence (Sloss, 1963, 1988), at least where that impinges upon the craton (Fedo and Cooper, 2001; Hogan et al., 2011; Keller et al., 2012). The lower member sits on an older sequence surface at the top of the Stirling Quartzite and is composed of several upward-shallowing parasequences (Fig. 3), three of which are capped by dolostones and have been widely used for correlation within the member (Stewart, 1966; Corsetti and Hagadorn, 2000; Nelson et al., 2023). Our compilation of the biostratigraphy is consistent with this approach (Supplemental dataset 1; but see Hogan et al., 2011).

In the coeval succession to the north, the 'White-Inyo facies' (Nelson, 1978), the equivalent units are the lower (Dunfee), middle (Esmeralda), and upper (Gold Point) members of the Deep Spring Formation, plus the underlying Reed Dolomite (Fig. 1; Cloud and Nelson, 1966; Alpert, 1974, 1975, 1976; Signor et al., 1987; Ahn et al., 2012; Smith et al., 2016). Stewart's (1966) long-standing lithological correlation of the Deep Spring Formation with the LMWCF has been supported by more recent geochemical and paleontological evidence (Corsetti and Kaufman, 1994; Corsetti and Hagadorn, 2000; Nelson et al., 2023; Smith et al., 2023).

Biostratigraphy. Horodyski's (1991) report of the discovery of the Ediacaran fossil *Ernietta* near the contact of the Wood Canyon Formation and Stirling Quartzite placed the Precambrian–Cambrian boundary within the lower part of the Wood Canyon Formation, and the subsequent discovery of *Treptichnus pedum* in the upper part of the lower member (Horodyski et al., 1994; Corsetti and Hagadorn, 2000; Hagadorn and Waggoner, 2000; Jensen et al., 2002; O'Neil et al., 2022) confined that transition to at or below the dolomite capping the second major parasequence of the lower member (Fig. 3; Supplemental dataset 1; Jensen et al., 2002). Although our reassignment of *Ernietta* to the new genus *Tulaneia* weakens the argument for an Ediacaran age for the basal part of the lower member, *Tulaneia* Runnegar and Horodyski n. gen. occurs with tubular body fossils (Fig. 4.5–4.8) that elsewhere in the LMWCF and in the Deep Spring Formation indicate an Ediacaran rather than a Cambrian age (Hagadorn and Waggoner, 2000; Smith et al., 2016, 2017; Selly et al., 2020). Furthermore, *Tulaneia* n. gen. is clearly an erniettomorph and therefore, by default, should be regarded as Ediacaran in age.
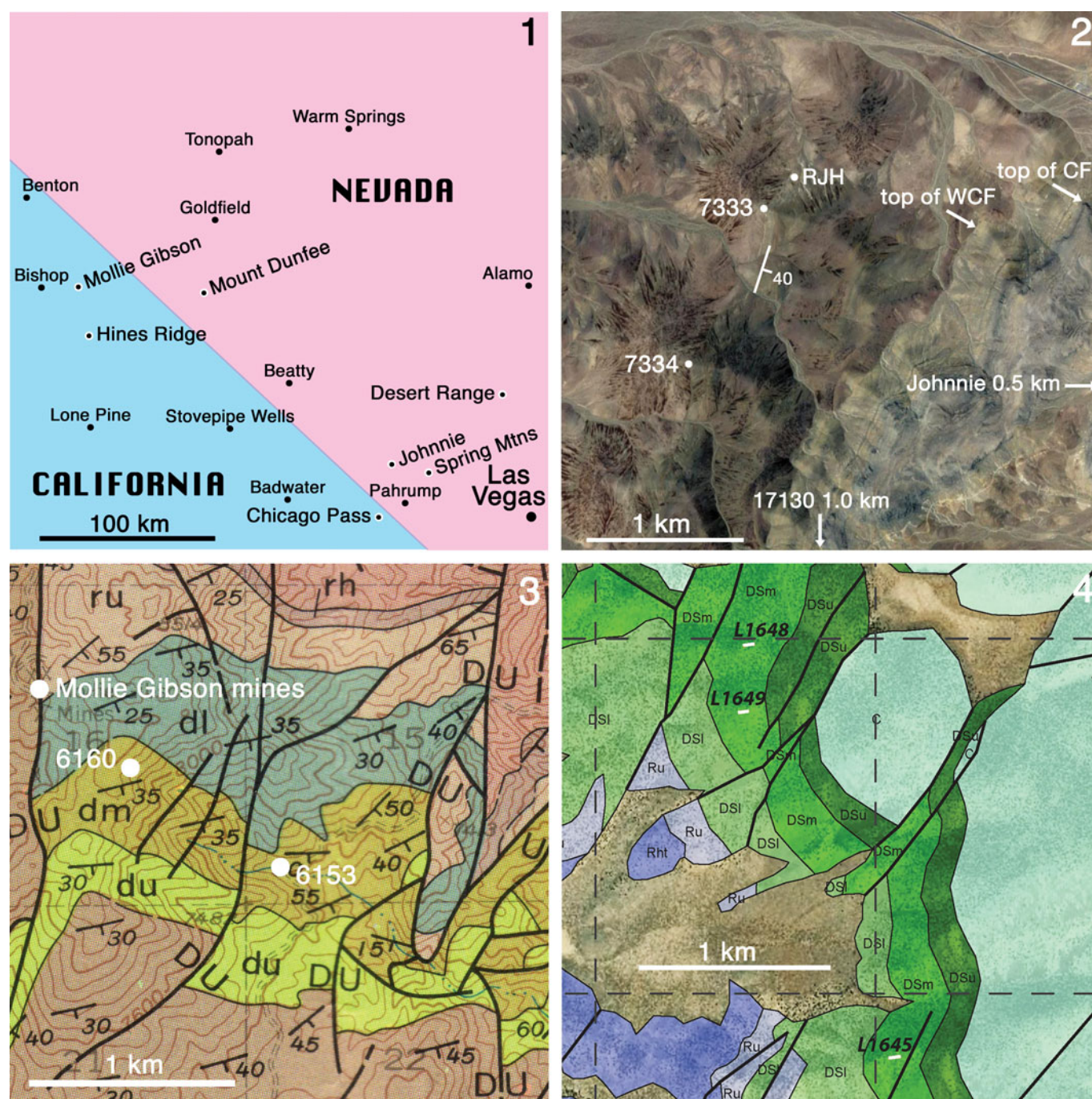
Figure 1. Locality maps. (**1**) Locations of fossiliferous sections of the middle (Esmeralda) member of the Deep Spring Formation (Mollie Gibson, Mount Dunfee), Wyman Formation (Hines Ridge), and the lower member of the Wood Canyon Formation (Desert Range, Johnnie, Spring Mountains, Chicago Pass) in California and Nevada. (**2**) Google Maps satellite image of the northern end of the Montgomery Mountains near Johnnie, Nevada, with UCLA localities 7333 and 7334 indicated by markers, near the bases of stratigraphic sections (Fig. 3) measured along the ridges extending to the ESE; RJH is Horodyski's discovery site (Fig. 4.3); 17130 refers to the location of LACNHM locality 17130 (Hagadorn and Waggoner, 2000, p. 359); WCF is Wood Canyon Formation and CF is Carrara Formation; as indicated, the investigated section has an average dip of about 40° SE. (**3**) Part of U.S.G.S. Geological Quadrangle Map Blanco Mountain (GQ-529; Nelson, 1966), republished with permission, showing UCLA fossil localities 6160 and 6153 in the Esmeralda (middle) Member (dm) of the Deep Spring Formation near the Mollie Gibson mines, White-Inyo Mountains. (**4**) Part of Nelson and Smith's (2019, DR-fig. 1) geological map of Mount Dunfee, Nevada, republished with permission, showing localities/sections (white rectangles) in the Esmeralda Member (DSm) of the Deep Spring Formation that have yielded *Psammichnites gigas arcuatus* (Fig. 12). Ru (ru) = upper member of the Reed Dolomite; rh = Hines Tongue of the Reed Dolomite; du = upper (Gold Point) member of the Deep Springs Formation; dl = lower (Dunfee) member of the Deep Springs Formation; DSl = Dunfee Member of the Deep Springs Formation; Dsu = Gold Point Member of the Deep Springs Formation; Rht = Hines Tongue of the Reed Dolomite.

Plagiogmus arcuatus Roedel, 1929, which now is considered a subjective junior synonym of *Psammichnites gigas* (Torell, 1868), is a distinctive, complex burrow system that is found in Fortunian and younger Cambrian strata in many parts of the world (Mángano et al., 2022). It was first reported as 'cf. *Pteridinium*' from the middle (Esmeralda) member of the Deep Spring
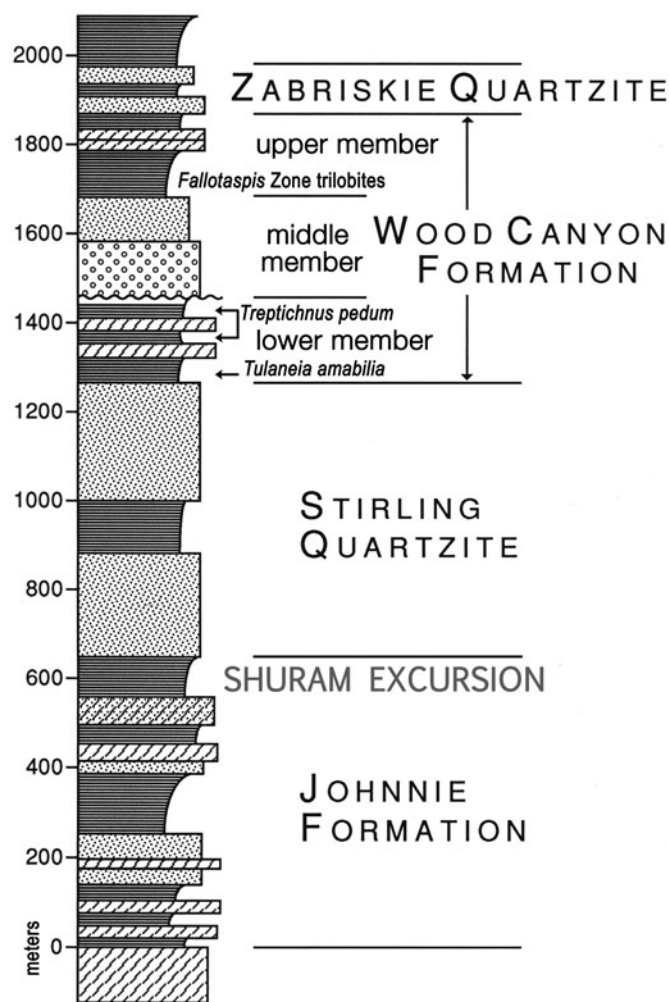
Figure 2. Summary of the stratigraphy enclosing the section of interest in the lower member of the Wood Canyon Formation, with the positions of the Shuram negative carbon isotope excursion and the oldest occurrence of Cambrian Stage 3 trilobites (*Fallotaspis* Zone trilobites) from Bergmann et al. (2011) and Hollingsworth (2011), respectively. The unconformity below the conglomeratic middle member of the Wood Canyon Formation is the base of the craton-wide Sauk megasequence (Sloss, 1963, 1988; Runnegar, 1998; Keller et al., 2012). Level of *Tulaneia amabilia* n. gen. n. sp. indicated in lower part of lower member, Wood Canyon Formation.

Formation in the White-Inyo mountains (Fig. 12.3; Cloud and Nelson, 1966, 1967), where it had been found by a graduate student named Cyril Gallick, who mapped an area immediately northwest of the discovery site (Gallick, 1964). Soon afterwards, Glaessner (1969, p. 390) questioned the proposed similarity to *Pteridinium* and suggested that Gallick's fossil could be a specimen of *Plagiogmus* that was "preserved in a thinner-bedded and more compacted rock and hence lack[s] the depth of tracks preserved in more massive and less compressible sandstone." Cloud and Bever (1973) accepted this suggestion and re-illustrated Gallick's specimen together with examples of *Plagiogmus* from Wyoming and South Australia. Based on four additional specimens found nearby (Fig. 12.2) and some others collected by J. Wyatt Durham (Durham, 1974), Alpert (1974, p. 74) felt that "the resemblance of Cloud's [sic] and Nelson's specimen to *Plagiogmus* may be fortuitous", a view shared by Nelson (1978), Jensen and Grant (1996), Runnegar (1998), Jensen et al. (2006), and Smith et al. (2023), but not by Durham (1974), Corsetti

and Kaufman (1994), Kaufman and Corsetti (1996), or O'Neil et al. (2022). Nevertheless, *Plagiogmus* has largely disappeared from the ichnofossil inventory of the White-Inyo succession (e.g., Mángano et al., 2022).

Ironically, the most convincing example is one of several similar specimens described by Nelson and Smith (2019, p. 909) as "microbially induced sedimentary structures" (MISS, Noffke, 2009). Nelson and Smith (2019, fig. 2A) illustrated two aligned, annulated burrows, one of which has the characteristic ladder-like ridges of *Plagiogmus* on its presumed original floor (Fig. 12.1). Several other specimens (Nelson and Smith, 2019, fig. 2; 2020, fig. 1) are far less like typical *Plagiogmus*, but may be interpreted as more or less intact burrows that have been deformed by soft-sediment movement after they were produced. As Glaessner (1969) had noted, most examples of *Plagiogmus* are preserved in medium- to coarse-grained sandstones and therefore resist compaction and other kinds of deformation. Apparently, this was not the case for the structures found at Mount Dunfee (Nelson and Smith, 2019), nor for the one from Cloud and Nelson's original locality (Glaessner, 1969; Alpert, 1974, pl. 5, fig. 11), both of which are found in finer-grained sediment. The preservation of the burrows is also complicated by superposition during dewatering (Fig. 12.4), which has led to interference patterns that apparently obscure the meandrine morphology that is typical of *Psammichnites gigas arcuatus* (Roedel, 1929), the type species of *Plagiogmus*. Additional confidence in the identification of the White-Inyo and Mount Dunfee structures as '*Plagiogmus*' comes from their almost exact stratigraphic equivalence in the middle part of the Esmeralda Member of the Deep Spring Formation (Cloud and Nelson, 1966; Nelson and Smith, 2019; Smith et al., 2023), and from the report of abundant *Plagiogmus* by Oliver (1990) from about the same stratigraphic position in the Mount Dunfee section as Nelson and Smith's (2019) MISS structures. There are, however, some significant differences between the '*Plagiogmus*' from the Deep Spring Formation and other early Cambrian examples of this ichnofossil; these discrepancies are discussed in the Systematic Paleontology section.

In the Mount Dunfee section, '*Plagiogmus*' occurs ∼435 m above the top of the Reed Dolomite (Nelson and Smith, 2019, fig. 1) at a level that is at or very near the peak (nadir) of the BACE negative carbon isotope excursion (Smith et al., 2016, 2023; Nelson et al., 2023). '*Plagiogmus*' is an iconic Cambrian ichnofossil and is not known from the Ediacaran, which means that the first appearance datum (FAD) for *Treptichnus pedum*—which has been used as a local standard for identifying the Ediacaran–Cambrian boundary in the Great Basin succession (Horodyski et al., 1994; Corsetti and Hagadorn, 2000; Jensen et al., 2002; Nelson et al., 2023; Smith et al., 2023)—may be just the start of the local stratigraphic range of *T. pedum* rather than the beginning of its biozone, and that the criterion for identifying the boundary in this region should now be supplanted by the FAD of '*Plagiogmus*' (i.e., *Psammichnites gigas arcuatus*). If that is done, the need to reduce the age of the Ediacaran–Cambrian boundary from ca. 539 to ca. 533 Ma (Nelson et al., 2023) goes away, because the nadir of the BACE excursion is ca. 539 Ma old in Sonora, Mexico (Hodgin et al., 2021; Nelson et al., 2023).

Chemostratigraphy and geochronology. In the White-Inyo successions, Deep Spring Formation carbonates yield the outlines of a significant negative carbon isotope excursion that has been identified as the basal Cambrian excursion (BACE; Corsetti and Kauffman, 1994; Corsetti and Hagadorn, 2003; Smith et al.,
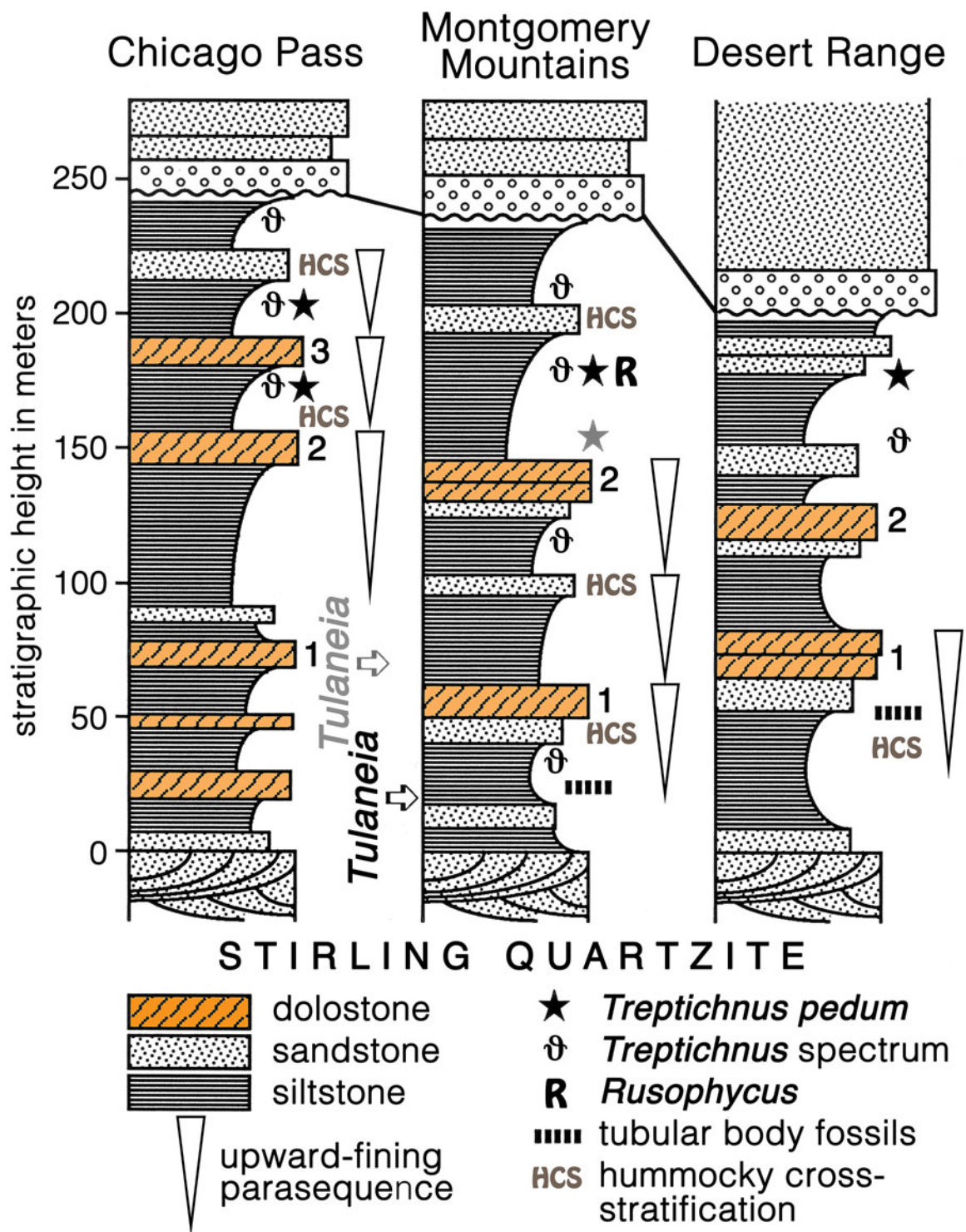
Figure 3. Cartoon representation of three sections measured by JGG through the lower member of the Wood Canyon Formation, simplified to emphasize major features of their lithostratigraphy and biostratigraphy and normalized to the top of the Stirling Quartzite; the three principal dolostone units are numbered 1, 2, and 3 and details are tabulated in Supplemental dataset 1; see text for explanation of 'Treptichnus spectrum traces.' Only some of the upward-fining parasequences are shown, but there are clearly more than the canonical 'three parasequences' (Corsetti and Hagadorn, 2000). The occurrences of Tulaneia n. gen. and Treptichnus shown in gray need further verification.

2016; Hodgin et al., 2021; Topper et al., 2022). The limited availability of carbonates in the Death Valley succession makes recognition of this event more difficult there, but the available data do support the traditional correlation of the Deep Spring Formation with the LMWCF (Corsetti and Hagadorn, 2003; Nelson et al., 2023; Smith et al., 2023).

The passive margin succession of the Great Basin has few volcanic flows or ash beds, but Nelson et al. (2023) found and dated
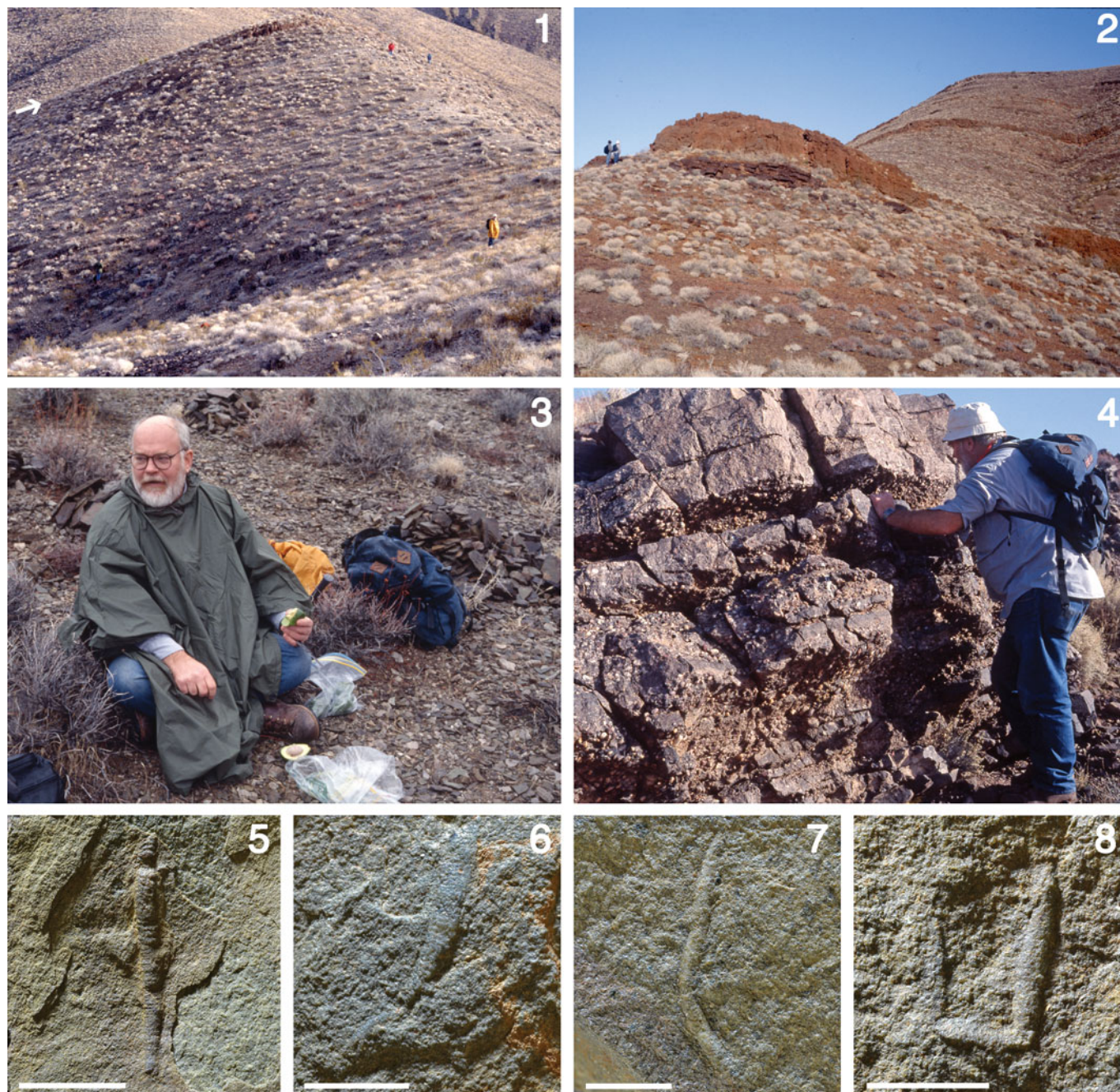
Figure 4. Outcrops (**1–4**) and annulated tubular body fossils (**5–8**). (**1**) Lower part of measured section at UCLA 7333 (Fig. 1.2) with RJH in yellow jacket standing on the dip slope at the top of the Stirling Quartzite; arrow indicates the outcropping edge of the first major dolostone (1, Fig. 3); (**2**) middle of the measured section at Chicago Pass at UCLA 7329 (Fig. 1.2), with JGG and RJH standing at the base of the second major dolostone (2, Fig. 3); the third major dolostone is visible in the distance; (**3**) Bob Horodyski, sitting at his discovery site in the Montgomery Mountains (RJH, Fig. 1.2) in 1993; the piles of slabs beside the pack and behind his head are two of several cairns that were constructed from pieces of float searched for fossils and now serve as permanent markers for the discovery site; (**4**) fluvial pebbly sandstone of the middle member of the Wood Canyon Formation being examined by RJH in the Nopah Range, south of Chicago Pass. (**5–8**) Poorly preserved tubular body fossils that retain some traces of closely spaced annulations (**5, 6**) and show some evidence for wall flexibility or fragility (**7, 8**), from beneath the first major dolostone of the lower member of the Wood Canyon Formation in the Spring Mountains (**5**, LACMIP 43368.1) and Montgomery Mountains (**6**, LACMIP 43369.13; **7**, LACMIP 43369.4; **8**, LACMIP 43369.12). All scale bars = 1 cm.

three successive ash beds in the upper part of the LMWCF in the Spring Mountains (Fig. 1.1) using the U–Pb ID-TIMS method. The ages range from 532.83 ± 0.98 to 531.32 ± 0.66 Ma and they embrace the section that, in the Montgomery Mountains and Nopah Range, contains the FAD of *Treptichnus pedum* (Supplemental dataset 1). For this reason, Nelson et al. (2023)

advocated elevating the age of the base of the Cambrian by ca. 6 Ma. However, for the reasons already discussed, this is not necessary; instead, the FAD of *T. pedum* in the LMWCF should be regarded as late Fortunian in age, according to recent estimates (533–530 Ma) of the age of the base of Cambrian Stage 2 (Bowyer et al., 2022, 2023; Hamilton et al., 2024).

Figure 5. *Tulaneia amabilia* Runnegar and Horodyski n. gen. n. sp., lowest part of lower member of the Wood Canyon Formation, RJH discovery site (Figs. 1.2, 4.3), Montgomery Mountains, Nevada. (**1**) Distal region of one of two specimens occurring on the surfaces of three small slabs (A–C) that fit together (**2**); (**2**) views of the edges and surfaces of three small slabs (A–C), found separately, but fit together and preserve parts and counterparts of the two best specimens: the holotype (**1, 2A, 2B**; LACMIP 43369.1A, LACMIP 43369.1B) and paratype (**2B, 2C, 5, 6**; LACMIP 43369.2A, LACMIP 43369.2B); (**3**) distal and proximal ends of two specimens, the larger of which is the counterpart of paratype LACMIP 43369.3B; (**4**) paratype LACMIP 43369.3A (part); (**5, 6**) broken edge of paratype LACMIP 43369.2A (part) showing clean sandstone filling tubular modules. Scale bars = 1 cm (**1**), 3 cm (**3–6**); 3-cm-grid squares (**2**).
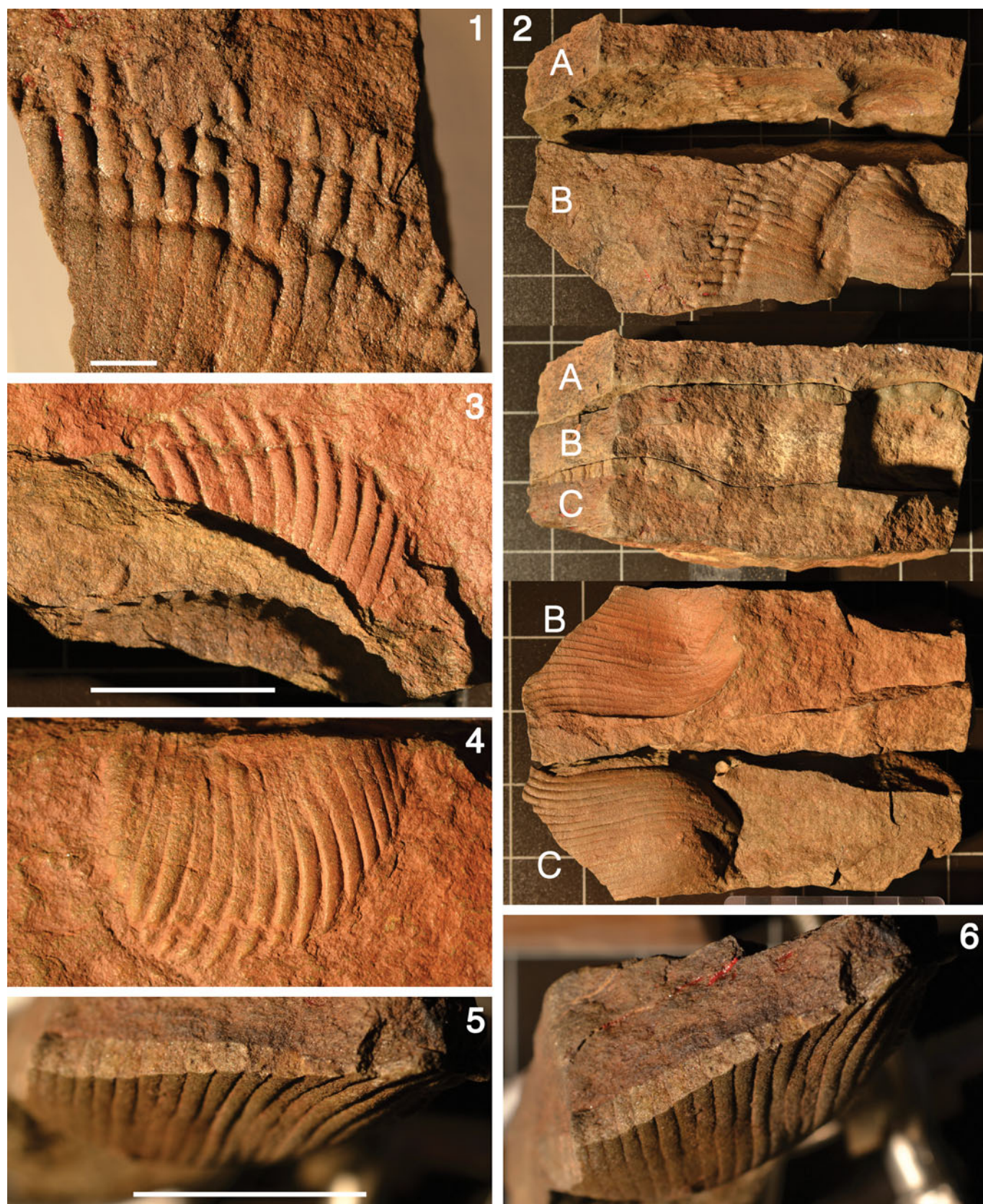
Figure 6. *Tulaneia amabilia* Runnegar and Horodyski n. gen. n. sp.: (**1–7**) Lowest part of lower member of the Wood Canyon Formation, RJH discovery site (Figs. 1.2, 4.3), Montgomery Mountains, Nevada, and *Pteridinium carolinaensis* (St Jean, 1973); (**8–10**), Nasep Member, Urusis Formation, UCLA 7322, Swartkloofberg farm, Namibia. (**1**) Front and side views of the holotype showing biplanar symmetry, clean quartzite filling, and absence of fill at the mid-height constriction, LACMIP 43369.1B (part); (**2**) two similar views of the distal end of paratype LACMIP 43369.2A (part) (also shown in Fig. 5.2B, 5.2C, 5.5, 5.6) at different focal planes to show the closely packed nature of the quartzite grains filling the modules; (**3**) oblique view of same specimen to show the parabolic cross section of the proximal end and the way the modules taper in thickness distally; (**4**, **5**), two similar specimens on the same slab: (**4**) the larger specimen, paratype LACMIP 43369.3, is illustrated in proximal view in (**5**) to show the flat iron-like termination of one module (black arrow) and the planar cracks that follow the originally organic module walls (white arrows); (**6**, **7**) part of paratype LACMIP 43369.3A (also shown in Fig. 5.4) showing views of the lateral surface and broken edge (part); (**8–10**) lateral and edgewise views of a quartz sandstone mold of a fragmentary specimen of *Pteridinium carolinaensis*, which preserves two of the three vanes, to illustrate a superficial similarity to *Tulaneia amabilia* Runnegar and Horodyski n. gen. n. sp. and a fundamental difference, in that there are no transverse partitions between the two vanes of *Pteridinium* (**9**), GSN F 1997. All scale bars = 2 cm.
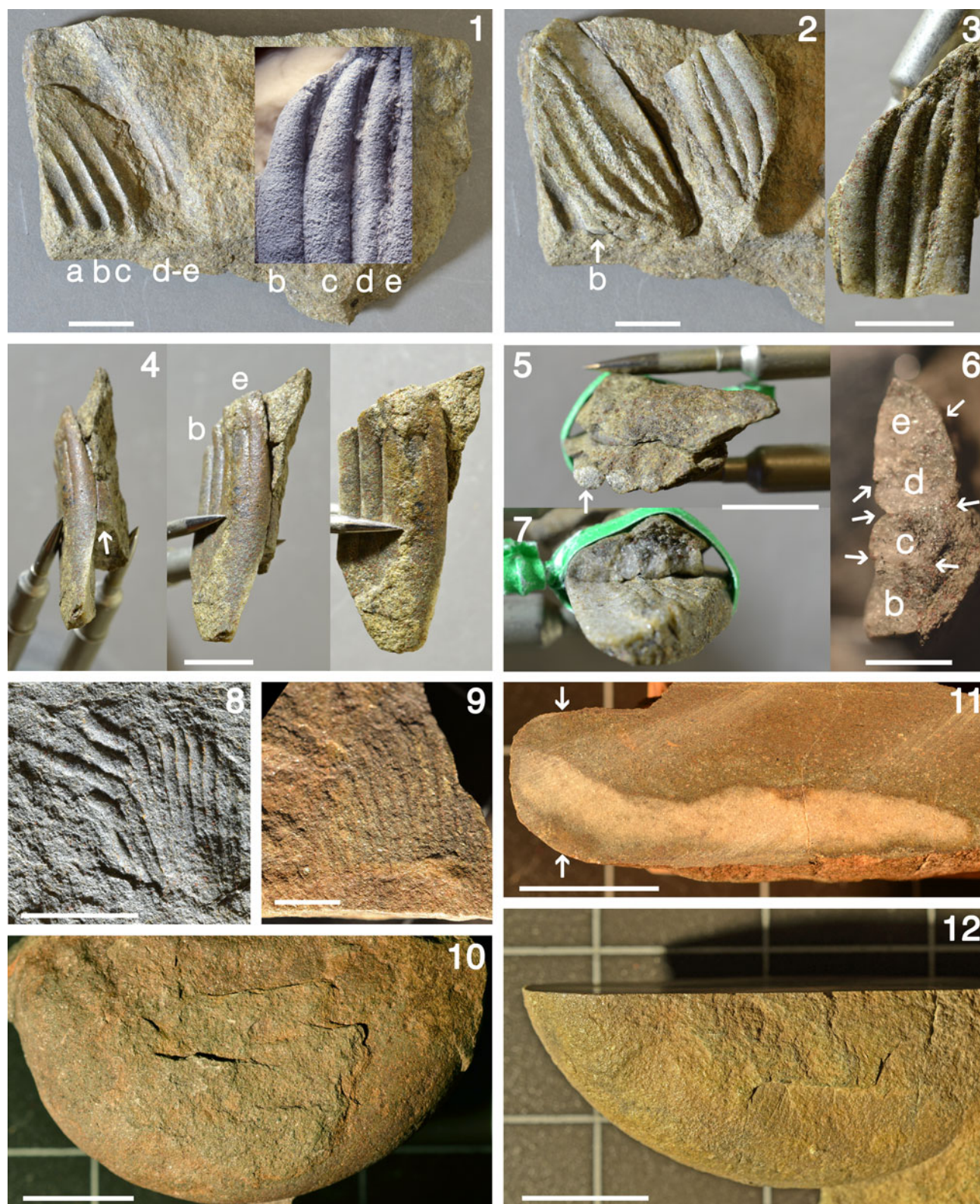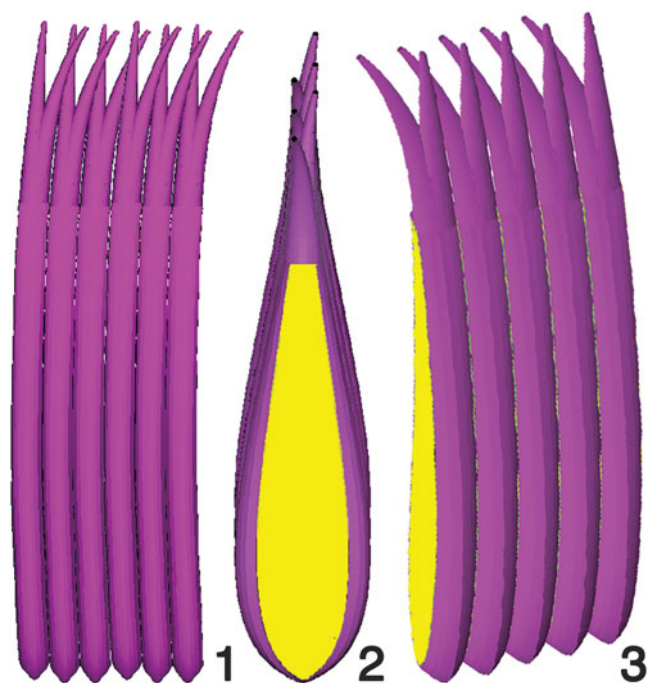
Figure 7. cont.

Figure 8. Three-dimensional model of several mature modules of *Tulaneia amabilia* Runnegar and Horodyski n. gen. n. sp. based on the holotype and paratypes, some artistic license and the assumption that the two sets of growing tips seen in paratype LACMIP 43369.6 (Fig. 7.1–7.6) are a feature of the organism, not an individual aberration such as a congenital abnormality. (**1**) Front view of model at right angles to plane of bilateral symmetry; (**2**) side view of model showing most of one septum (yellow/light area); (**3**) oblique view of back of model.

Stratigraphic information. See Figures 2–4, Appendix 1, Supplementary dataset 1, and the discussion under Materials and methods.

Locality information. RJH used his own numbering system based on his initials and date of collection (e.g., RH-91-8-19-1) and recorded site information in his field notebooks: https://sova.si.edu/record/sia.fa16-098. We used the UCLA locality numbering system (e.g., UCLA 7333) for sites, occasionally at the same place in stratigraphic order, and numbered each piece of rock collected accordingly. Important fossils were then given decimal numbers (e.g., 7333.1, 7333.2, etc.). Pieces of an individual fossil and parts and counterparts were given the same decimal number

and then distinguished by letters (e.g., 7333.1A, 7333.1B, etc.). Those UCLA numbers for individual fossils were replaced by Los Angeles County Museum Invertebrate Paleontology (LACMIP) locality numbers (e.g., LACMIP 43369), specimen numbers (e.g., LACMIP 43369.1), and type numbers (e.g., LACMIP Type 15019) after the collection was donated to the Museum, but the UCLA locality numbers (e.g., UCLA 7307) still pertain and are used in the figures, Appendix 1, and Supplemental dataset 1. All collection numbers associated with type specimens are listed for clarity and in order to maintain specimen provenance; locality information is tabulated in Supplemental dataset 1 and the localities are described in Appendix 1. Because this work was carried out before GPS became widely available, the geographic positions of localities were plotted on road and topographic maps of various sources and scales. These map records were used recently to find the exact locations of the sites on Google Maps and to obtain their decimal longitudes and latitudes (Fig. 1; Appendix 1); Google Maps uses the WGS84 standard.

Materials and methods

All of the material used for this study was obtained during field work carried out in 1993 and 1995. Stratigraphic sections were measured using a Jacob staff or a measuring tape. There are, however, some discrepancies between our measurements and those of others who have studied the same sections (Supplemental dataset 1), presumably because of differences in estimates of average dip, which varies significantly from place to place.

Preparation of the fossils has been minimal. Field photographs and images of specimens taken during the 1990s were made with a Minolta X700 35 mm FSLR camera equipped with Minolta MC Macro Rokkor-QF 50 mm lens using Kodak Ektachrome Professional film. Color slides and negatives were digitized using an Epson Perfection V700 Photo scanner. Digital images, taken more recently, were made with a Nikon D3100 DSLR camera equipped with Nikon AF-S Micro Nikkor 40 mm lens. Preparation of the figures was carried out with Adobe Photoshop, Adobe Illustrator, and Aldus Super3D.

Repositories and institutional abbreviations. Figured and other specimens examined or mentioned in this study are deposited in the following institutions: Natural History Museum of Los Angeles County, Invertebrate Paleontology, Los Angeles (LACMIP); South Australian Museum, Adelaide, Australia

Figure 7. *Tulaneia amabilia* Runnegar and Horodyski n. gen. n. sp. (**1–9**) and two possible taphomorphs of *T. amabilia* Runnegar and Horodyski n. gen. n. sp. (**10–12**), all except (**8**) from the lowest part of the lower member of the Wood Canyon Formation at the RJH discovery site (Figs. 1.2, 4.3), Montgomery Mountains, Nevada; (**8**) is from ~14 m above the base of the Wood Canyon Formation on the opposite (south) side of the ridge used to measure section 7333 (Fig. 1.2). (**1–6**) Several images of three small pieces (A–C), found separately by RJH (B and C) and KJP (A), but which proved to fit together as counterpart A (**1**, left), part B (**4**, right), counterpart C (**2**, left), and part D (**1**, right; **2**, right; **3**) to form paratype LACMIP 43369.6; three pieces (B–D) of paratype LACMIP 43369.6 are assembled in (**4**), (**5**), and (**7**) and their original biological continuity is best illustrated by the smooth curved external surface that connects part A with part C (**4**, arrow). (**1**) Small slab that has cast three equal-sized tubular modules (a–c) and one of double width (d–e) that is divided on the opposite side of the organism, paratype LACMIP 43369.6A (counterpart); insert shows a view of part C that has been whitened with ammonium chloride for comparison with (**3**); (**2**) all three fragments juxtaposed, with part B and counterpart C lying in place on counterpart A, and part D inverted on counterpart A to the right; the end of the b module of part B is just visible (arrow), paratype LACMIP 43369.6A–D; (**3**) unwhitened view of part C for comparison with the insert in (**1**), paratype LACMIP 43369.6C; (**4**) three views of the assembled parts B through D showing two tubular modules (b and c) and one of double width (d + e) on the counterpart A side of the organism, paratype LACMIP 43369.6B–D; (**5**) view of distal end of the assembled parts B through D with the b module of part B indicated by the arrow, paratype LACMIP 43369.6B–D; (**6**) proximal view of the broken edge of part D showing cross-sections of four modules and the positions of the three intervening walls (arrows), paratype LACMIP 43369.6D; (**7**) view of the proximal end of the assembled parts B through D showing a wide flat surface that represents the unseparated d + e modules of part B, paratype LACMIP 43369.6B–D; (**8, 9**) fragments of poorly preserved specimens of *Tulaneia* n. gen. that have more stratigraphic than biological significance, having been found at approximately the same level on opposite sides of the ridge section UCLA 7333 (Fig. 1.2) LACMIP 43369.5 and LACMIP 43369.11, respectively; (**10–12**) two similar sized concretion-like structures that may represent inflated taphomorphs of the outer wall of an ernietromorph such as *Tulaneia* n. gen.; the one that has been sectioned has a volume of quartzite that may reflect an earlier filled shape, LACMIP 43369.10 (**10**) LACMIP 43369.9 (**11, 12**). Scale bars = 5 mm (**6**), 1 cm (**1–5, 7–9**), and 2 cm (**10–12**).
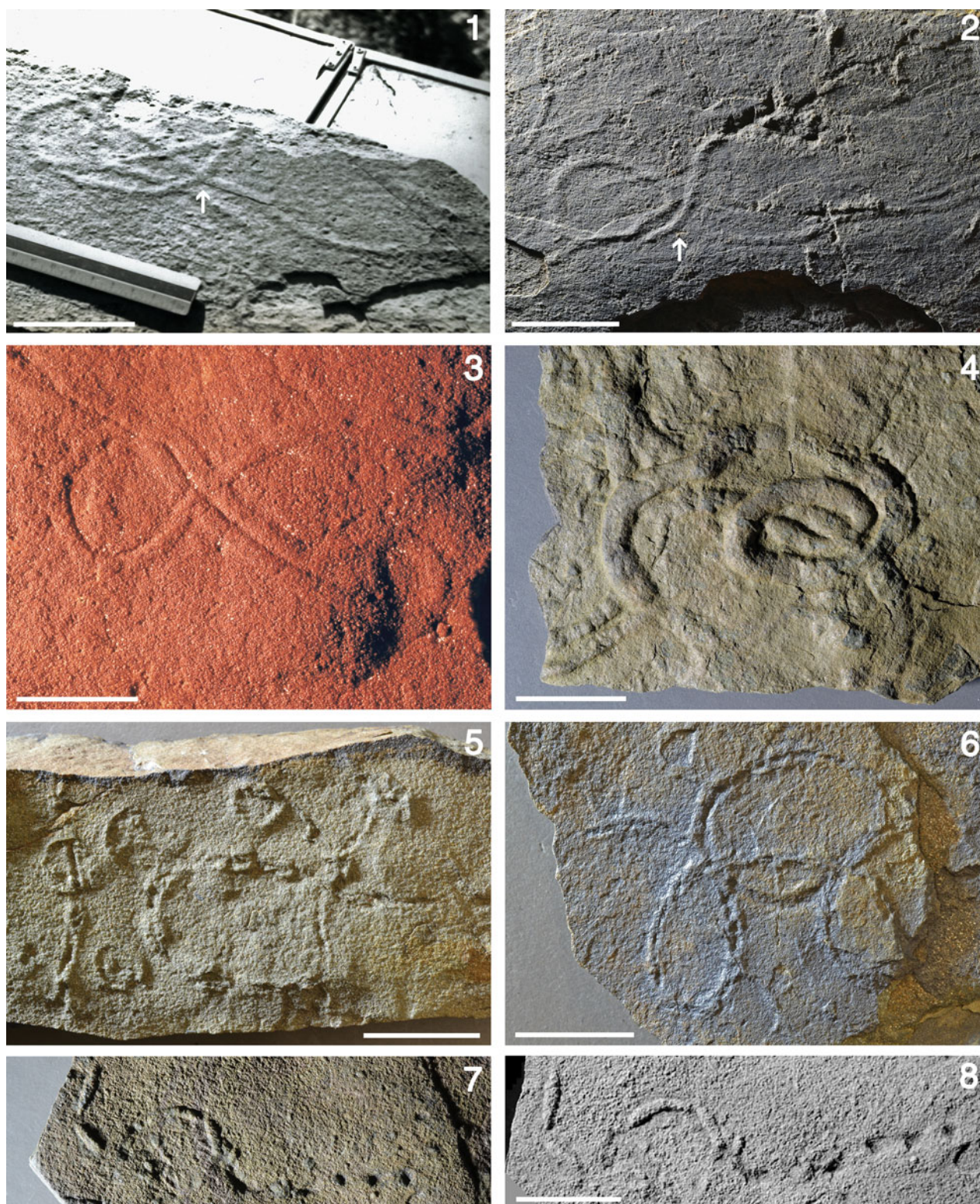
Figure 9. Looped structures (body fossils or trace fossils) that have constant widths/diameters and are preserved in convex hyporelief from the Wyman Formation at Hines Ridge, California (**1, 2**), the Ediacara Member of the Rawnsley Quartzite at Ediacara, South Australia (**3**), and the lower member of the Wood Canyon formation in the UCLA 7334 section, Montgomery Mountains, Nevada (**4**), as well as bed-base traces of the *Treptichnus* spectrum, all from the lower member of the Wood Canyon Formation (**5–8**). (**1**) Backyard photograph of a specimen collected prior to November 1970 by Langille (1974) and reported anecdotally in the literature since then; (**2**) a specimen found by BR in 1988 that is similar in size and topology (arrows) to Langille's tentatively identified as the ichnotaxon ?*Gordia* isp. (**1**), LACMIP 43374.1; (**3**) a comparable looped hyporelief structure from an Ediacara Member flagstone, previously illustrated as the bilaterian trace fossil *Gordia* isp. (Runnegar and Fedonkin, 1992, fig. 7.6.3C), SAM P27977; (**4**) a float specimen from UCLA 7334 that, perhaps, is more confidently identified as the trace fossil *Gordia* isp. rather than a body fossil, LACMIP 43372.1; (**5**), a specimen found by RJH in 1991 that, according to him, came from ~10 m above the *Tulaneia* n. gen. horizon in the 7333 section (Supplemental dataset 1), LACMIP 43369.15; (**6**) another specimen from the RJH collection at an unrecorded level in the 7333 section that is similar to (**5**) but may be more confidently be referred to *Treptichnus* isp., LACMIP 43369.16; (**7, 8**) unwhitened and whitened images of a trace from the 203 m level in the Chicago Pass section, UCLA 7329, showing behavior that is approaching that of bona fide *Treptichnus pedum* (Fig. 10.8), LACMIP 43370.1. Scale bars = 5 cm (**1, 2**) and 2 cm (**3–8**).
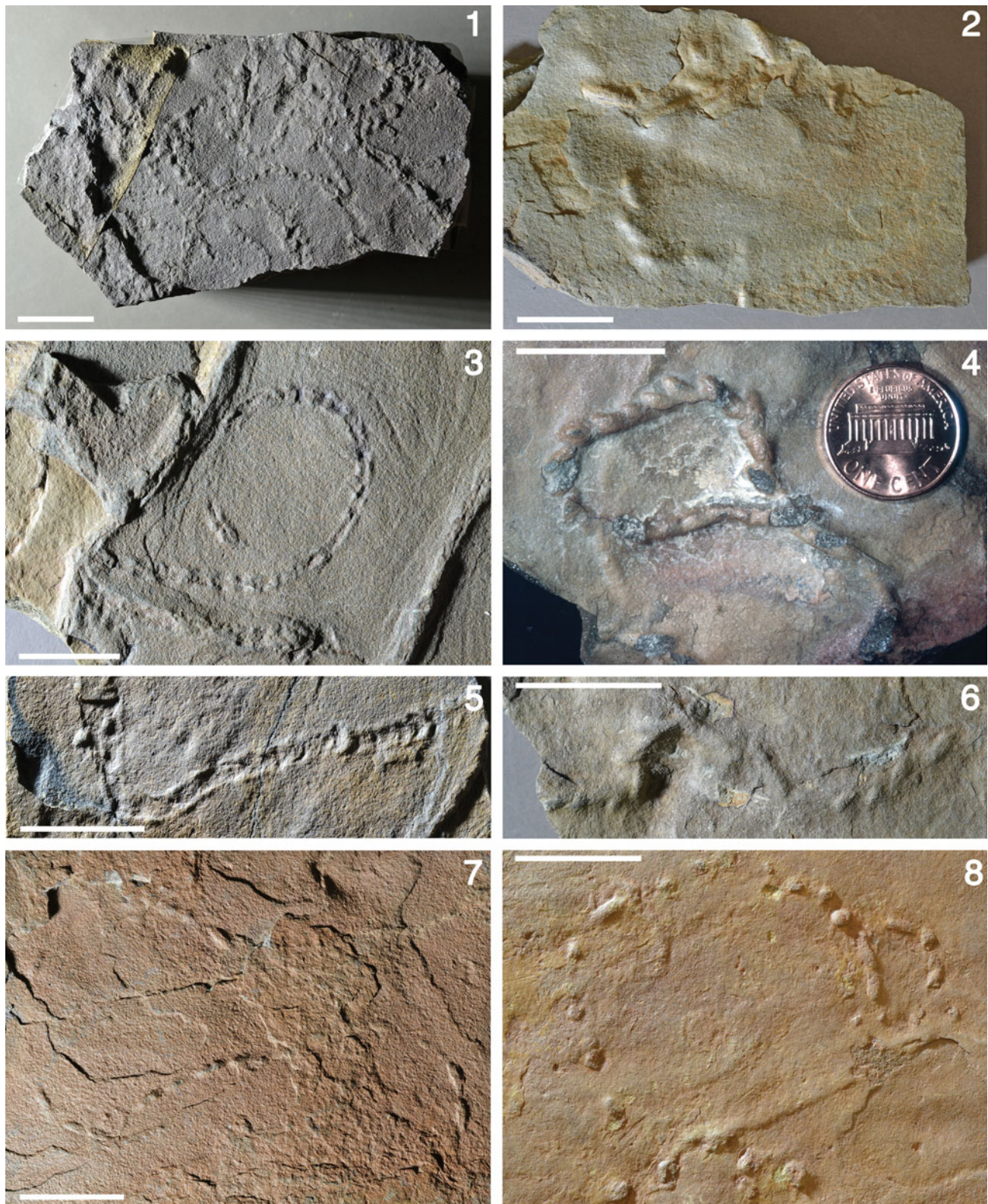
Figure 10. *Treptichnus* isp. cf. *T. pedum* (Seilacher) from the lower member of the Wood Canyon Formation in the Desert Range and Montgomery Mountains (**1**, **3**) and *Treptichnus pedum* from the lower member of the Wood Canyon Formation in the Montgomery Mountains (**2**, **4**, **6**), Chicago Pass (**7**), and the Nomtsas Formation, Sonntagsbrunn farm, southern Namibia (**8**). (**1**) Bed-base traces from a level with numerous similar structures that collectively can be identified as *Treptichnus* spectrum (Fig. 3), LACMIP 43371.1; (**2**) RJH sample from an unrecorded level within the lower member of the Wood Canyon Formation but probably from the same horizon as UCR 10703/1 (Jensen et al., 2002, fig. 4B), LACMIP 43369.17; (**3**) one of several structures (Figs 8.5, 8.6, 8.7, 8.8, 10.5, 10.6) that grade between *Treptichnus* and *Gordia* in continuity of the trace and geometry of its trajectory, LACMIP 43369.20; (**4**) iconic example of *T. pedum* found by MJV in float between the second and third major dolostones, LACMIP 43372.5; (**5**) enlarged view of a segmented trace that falls well within the *Treptichnus* spectrum shown in Figure 11.7, LACMIP 43369.18; (**6**) another iconic example of *T. pedum* with better stratigraphic control (Supplemental dataset 1), LACMIP 43369.19; (**7**, **8**) comparable specimens of *T. pedum* from Nevada and Namibia, LACMIP 43370.2 and GSN F 1952, respectively. All scale bars = 2 cm.
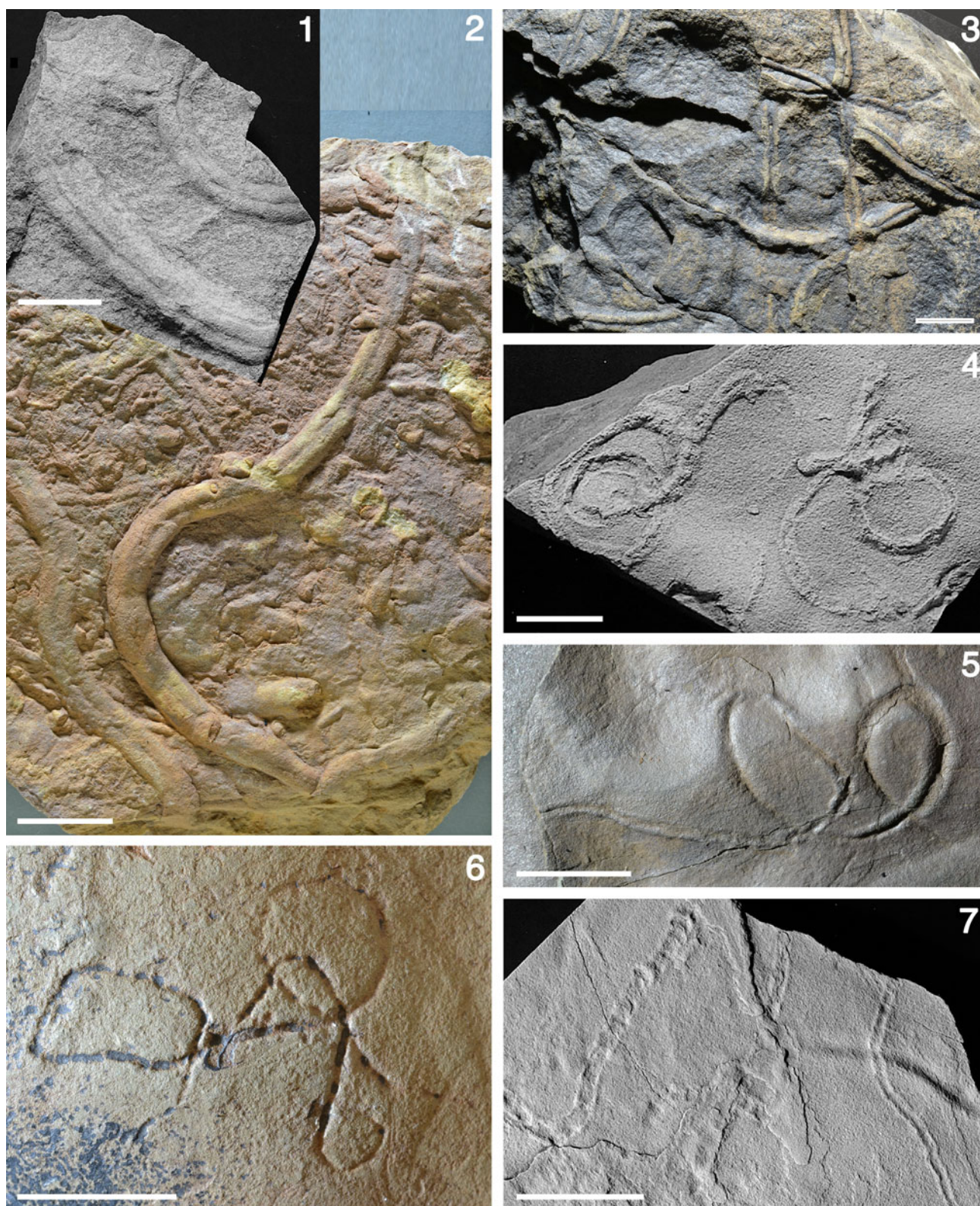
Figure 11. *Didymaulichnus miettensis* Young (**1–3**) from the lower member of the Wood Canyon Formation, Chicago Pass and Montgomery Mountains, California (**1**, **3**) and Member IV, Arumbera Formation, Ross River, Northern Territory, Australia (**2**), plus looped trace fossils (**4**, **5**) and *Treptichnus* spectrum traces (**6**, **7**) from the lower member of the Wood Canyon Formation, Nevada. (**1**) Small piece, found in situ at ~200 m (Supplemental dataset 1), showing parts of three curved traces, LACMIP 43370.3; (**2**) longer, similar traces from the Arumbera Formation, Australia, also preserved in convex hyporelief, LACMIP 43373.1; (**3**) sandstone joint block with several hyporelief traces, previously illustrated by Jensen et al. (2002, fig. 5A), LACMIP 43369.20; (**4**) two looped traces that show features of both *Gordia* and *Didymaulichnus*, bed base whitened with ammonium chloride, LACMIP 43369.2; (**5**) looped trace on upper bed surface at 95 m, closely comparable to *Psammichnites gigas circularis*, LACMIP 43372.3; (**6**) looped trace that is intermediate between *Treptichnus* and *Gordia*, found in situ 6–7 m below third major dolostone (Supplemental dataset 1), LACMIP 43372.4; (**7**) two *Treptichnus* spectrum traces on a small slab, whitened with ammonium chloride from ~150 m, LACMIP 43369.18. All scale bars = 2 cm.

Figure 12. *Psammichnites gigas arcuatus* (Roedel), Esmeralda Member, Deep Spring Formation at Mount Dunfee, Nevada (**1**, **5**) and Mollie Gibson, White-Inyo Mountains, California (**2**, **3**); Member IV, Arumbera Sandstone, Ross River, Northern Territory, Australia (**4**); and File Haidar Formation, Sweden (**6**). (**1**) Least-deformed and therefore most recognizable of 'problematic corrugated tubular structures' illustrated by Nelson and Smith (2019, p. 911, fig. 2A, republished with permission); arrow indicates presumed wall of burrow for comparison with (**2**); (**2**) two of four additional specimens of 'cf. *Plagiogmus*' UCLA 49569 and UCLA 49570, now LACMIP 26153.1 and LACMIP 26160.1, respectively from Alpert (1974, pl. 5, figs 3, 4, republished with permission) UCLA localities 6153 and 6150 (Fig. 1.3), showing corrugation of both upper (arrow) and lower surfaces of the burrow; (**3**) specimen found by Cyril Gallick ~600 m SE of the Mollie Gibson mines (Fig. 1.3; Cloud and Nelson, 1966, fig. 3D), LACMIP 16338.1 ex UCLA 45726; (**4**) sandstone cast of lower surface of a complete burrow with a characteristic sinuous groove on the upper surface (not shown), LACMIP 43373.2; (**5**) upper surface of sizeable slab described as "bifurcating ripples with corrugations" by Nelson and Smith (2019, p. 912, fig. 4A, republished with permission), with one superimposed crossover indicated by arrow; (**6**) inverted image of a photograph provided by Anders Martinsson of the bases of 'empty' burrows, cast in sandstone, with regularly spaced transverse ridges caused by peristaltic contractions of the producers, SMNH X2074 (Jaeger and Martinsson, 1980, fig. 2). All scale bars = 3 cm.

(SAM); Swedish Museum of Natural History, Stockholm, Sweden (SMNH); Faculty of Geology Museum, University of Oveido, Spain (AMC); Department of Earth and Planetary Sciences, University of California, Riverside, California (UCR). Locality information is registered with the Department of Earth, Planetary, and Space Sciences, University of California, Los Angeles (UCLA), Los Angeles, U.S.A., the Natural History Museum of Los Angeles County, Invertebrate Paleontology, Los Angeles (LACMIP or LACNHM), the Department of Earth and Planetary Sciences, Johns Hopkins University, Baltimore (JHU) and the School of Environmental and Rural Science, University of New England, Armidale, Australia (UNE).

Systematic paleontology

<div align="center">

Class **Erniettomorpha** Pflug, 1972
Family **Erniettidae** Pflug, 1972
Genus *Tulaneia* Runnegar and Horodyski new genus

</div>

Type species. *Tulaneia amabilia* n. gen n. sp. from the lower member of the Wood Canyon Formation, Montgomery Mountains, Nevada.

Diagnosis. As for the type species by monotypy.

Occurrence. Lower member, Wood Canyon Formation, Nevada, U.S.A. (Horodyski, 1991; Horodyski et al., 1994; Smith et al., 2017, 2023).

Etymology. Named for Tulane University, New Orleans (formerly the University of Louisiana) for its role in encouraging and supporting research in paleontology and other areas of natural history as exemplified by the distinguished careers of Robert J. Horodyski, Alfred R. Loeblich and Helen Tappan Loeblich, Ronald L. Parsley, Harold E. and Emily H. Vokes, and Shuhai Xiao.

Remarks. *Tulaneia* n. gen. resembles *Ernietta* Pflug (1966) in being constructed from a stockade of tubular modules but differs in having only a single, fan-shaped array, rather than being shaped like a sack. Because there are two sets of growing tips on one of the paratype specimens (Figs. 7.1–7.6, 8), it was originally thought to have a sack-shaped body that was flattened during burial and compaction. Closer inspection of the paratype revealed that the modules in this specimen bifurcate near their growing tips (Fig. 7.4) and do not, therefore, represent two sides of a sack-shaped organism. This terminal bifurcation is thought to be a property of the organism rather than a developmental abnormality, although the latter possibility cannot be excluded.

<div align="center">

Tulaneia amabilia Runnegar and Horodyski new species
Figures 5, 6.1–6.7, 7.1–7.9, 7.11, 7.12?, 8

</div>

1991   *Ernietta* Pflug; Horodyski, p. A163.
1994   *Ernietta plateauensis* Pflug; Horodyski et al., p. 60.
1998   erniettid Ediacaran; McMenamin, p. 30, fig. 2.16.
2017   *Ernietta* Pflug; Smith et al., p. 4, fig. 3a–h.
2020   erniettomorph; Hall et al., p. 2, fig. 1b.
2022   *Ernietta plateauensis* Pflug; Runnegar, p. 1104, fig. 3a.

Holotype. Part (RH-91-8-19-1/UCLA 7331.1B/LACMIP 43369.1A LACMIP Type 15019) and counterpart (RH-91-8-19-1/UCLA 7331.1A/LACMIP 43369.1B LACMIP 15019) preserved on two of three stratigraphically contiguous thin sandstone slabs (Fig. 5.2) from the lowest 10–20 m of the lower member of the Wood Canyon Formation at the discovery site (RJH, Fig. 1.2), northwest of Johnnie, Nevada; the part preserves a clean quartzite filling of the modules (Fig. 6.1).

Paratypes. Paratype, part (RH-91-8-19-1/UCLA 7333.1C/LACMIP 43369.2A LACMIP Type 15020) and counterpart (RH-91-8-19-1/UCLA 7333.1B/LACMIP 43369.2B Type 15020) preserved on the second and third slabs of the three stratigraphically contiguous slabs that also preserve the holotype (Fig. 5.2); paratype, larger of two individuals on another slab (RH-92-1-12-1/UCLA 7333.2/LACMIP 43369.3 LACMIP Type 15021; Fig. 6.4), also filled with quartzite (Fig. 6.5); paratype, part (UCLA 7333.3B/LACMIP 43369.4A LACMIP Type 15022) and counterpart (UCLA 7333.3A/LACMIP 43369.4B LACMIP Type 15022) of the distal half of a specimen that is partially filled with clean quartzite (Fig. 6.7); paratype, three small separate pieces that fit together and preserve the counterpart (UCLA 7333.5A/LACMIP 43369.6A LACMIP Type 15023; Fig. 7.1), part and counterpart (RH-91-8-17-1/UCLA 7333.5B/LACMIP 43369.6B–C LACMIP Type 15023; Fig. 7.2), and part (RH-91-8-16-1/UCLA 7333.5C/LACMIP 43369.6D LACMIP Type 15023; Fig. 7.3) of the tips of two sets of quartzite-filled modules (Fig. 7.1–7.6).

Diagnosis. Decimeter-scale lyre-shaped organism composed of unmineralized tubular modules arranged side-by-side like a palisade and separated by planar partitions; modules are wide near the proximal edge of the body, diminish in size gradually in the distal direction, and then separate laterally and taper to blunt points at their distal terminations; duplication of the tips of the modules has been observed in one case.

Description. Body lyre-shaped, composed of as many as ~30 tubular modules in complete specimens, arranged side-by-side in a palisade fashion, and which join proximally in an acutely rounded margin; body cross section is bilaterally symmetrical with maximum width near the proximal margin and minimum width at tapered distal terminations; profile at right angles to the proximal margin is lyre-shaped and parallel to the margin; it is aerodynamic (streamlined); modules are largest at the mid-line, up to ~5 mm width near the proximal margin and up to ~9 mm in depth perpendicular to the margin, and they diminish gradually in size in both directions away from the axis; lateral limits of body not well preserved/exposed; one three-dimensional specimen has modules with bifurcated distal tips, which may or may not be a general property of the organism.

Etymology. From *amabilis*, Latin, lovely, in reference to the exquisite preservation of the type material.

Taphonomy. All of the type specimens of *Tulaneia* n. gen. were completely or partially filled with clean quartz sand prior to burial (Figs. 5.5, 5.6, 6.1–6.3, 6.5, 6.7, 7.5–7.7), as was one of the associated 'taphomorphs' (Fig. 7.11). The obvious contrast between the clean fillings and their surrounding silty matrices is an indication that the internal cavities of *Tulaneia* n. gen. were loaded with suspended quartz grains, either in a high-energy shoreface environment like that of the underlying Stirling Quartzite (Smith et al., 2017), or during onshore to offshore transport via storm surge activity. As a result, the bodies of *Tulaneia* n. gen. seem to have behaved like sandbags during transport and were deposited with

cobbles (Smith et al., 2017) in deeper water environments. As in Namibia and South Australia, erniettomorphs (*Ernietta*, *Pteridinium*, and *Tulaneia* n. gen.) are rarely if ever preserved in the environments in which they lived (Runnegar et al., 2024).

Remarks. A cluster of distorted specimens of *Tulaneia amabilia* n. gen. n. sp. discovered by Smith et al. (2017) in the vicinity of LACNHM locality 17130 (Fig. 1.2) are similar in shape, size, and preservation to the material from the Horodyski site (RJH, Fig. 1.2). However, one of their specimens (Smith et al., 2017, fig. 3a, b, e, f) was thought to show a suture of the kind found in *Ernietta*, which has a zig-zag seam between opposite sides of the body (Ivantsov et al., 2016). Close inspection of the published images suggests that the 'suture' is due to a fortuitous juxtaposition of two individuals, with the proximal margin of one nearly aligned with the proximal margin of the other. In this interpretation, the proximal margin of the larger of the two individuals is fully exposed whereas the proximal margin of the smaller individual abuts the wall of the larger one at some distance from its proximal margin. Although this configuration could possibly be explained by budding (asexual reproduction), sedimentary stacking during deposition is our preferred hypothesis.

Several puck-shaped structures, one of which is partially filled with clean quartzite, were also found at RJH's discovery site (Fig. 7.10–7.12) and contributed to the erroneous identification of *Tulaneia* n. gen. as *Ernietta*. Circumstantial evidence based on their co-occurrence suggests that these and similar objects found by Smith et al. (2017) may be the distended exterior walls of individuals of *Tulaneia* n. gen. or perhaps another eriettomorph. Some of the structures reported by Smith et al. (2017) showed traces of fine or coarse ribbing and were regarded as 'taphomorphs' of the better-preserved body fossils (Hall et al., 2020). We concur with that suggestion.

Ichnofossils

Remarks. Ichnofossils have been instrumental in attempts to place the Ediacaran–Cambrian boundary in both the White-Inyo and Death Valley regions of the Great Basin for almost 60 years (Cloud and Nelson, 1966; Glaessner, 1969; Cloud and Bever, 1973; Langille, 1973, 1974; Alpert, 1974, 1975, 1976; Durham, 1974; Nelson, 1978; Oliver, 1990; Horodyski et al., 1994; Runnegar, 1998; Corsetti and Hagadorn, 2000, 2003; Jensen et al., 2002; Oliver and Rowland, 2002; Smith et al., 2017, 2023; Tarhan et al., 2020; O'Neil et al., 2022). Here we focus on three kinds of ichnofossils, selected for their paleoenvironmental significance and biostratigraphic importance: (1) looped structures (Fig. 9.1, 9.2; Langille, 1973, 1974), either body or trace fossils, from the Wyman Formation at Hines Ridge (Fig. 1.1) in the White-Inyo facies; (2) traces of the *Treptichnus* spectrum (Figs 9.5–9.8, 10.1, 10.3, 10.7, 11.5, 11.6), including bona fide examples of *Treptichnus pedum* (Seilacher, 1955) (Fig. 10.2, 10.4; Jensen et al., 2002) and *Didymaulichnus miettensis* Young, 1972 (Fig. 11.1–11.3; Jensen et al., 2002), from the lower member of the Wood Canyon Formation in the Death Valley facies; (3) *Psammichnites gigas arcuatus* (Roedel, 1929) (Fig. 12.1–12.3, 12.5; Cloud and Nelson, 1966; Alpert, 1974; Nelson and Smith, 2019) from the Esmeralda Member of the Deep Spring Formation in the White-Inyo facies.

Looped structures (trace or body fossils)
Figure 9.1–9.4

Description. Poorly preserved, apparently cylindrical structure at least ~50 cm in length and 5 mm in width that makes one complete loop of ~5 cm diameter.

Material. LACMIP 43374.1, slab of slate from the upper Wyman Formation, Hines Ridge, California (Fig. 1.1).

Remarks. In 1970, Gerry Langille, then a graduate student at SUNY Binghamton (now Binghamton University), sent Clem Nelson a field photograph of a similar trace that he found in the Wyman Formation; Nelson passed that photograph on to BR in ca. 1988 and it is reproduced here (Fig. 9.1). Our specimen closely resembles Langille's in dimensions and topology, with similar crossings (indicated by arrows in Fig. 1.1 and 1.2). A third, possibly similar specimen, was illustrated by Corsetti and Hagadorn (2003, fig. 5A) as *Helminthoidichnites* but with the proviso that "we cannot falsify the hypothesis that some of these are body fossils" (Corsetti and Hagadorn, 2003, p. 6).

Runnegar and Fedonkin (1992, fig. 7.6.3C) illustrated a comparable structure from the base of a bed at Ediacara, South Australia, which they confidently identified as the trace fossil *Gordia* isp. We refigure that specimen (Fig. 9.3) in order to illustrate its similarity to the Wyman structures but note that it is no longer possible to be confident that it is a trace fossil rather than a body fossil. The new understanding that followed discoveries of numerous tubular body fossils in the Ediacaran of Namibia (Budd and Jackson, 2015; Schiffbauer et al., 2016; Darroch et al., 2018; Chai et al., 2021; Runnegar et al., 2024) and elsewhere, make it equally likely that the Wyman structures, and the one from Ediacara, are body fossils rather than traces, although the half-meter length of the former would be extraordinary for a tubular body fossil (but see Bobrovskiy et al., 2022, fig. S1). Another similar structure from the LMWCF (Fig. 9.4) is more confidently identified as the ichnofossil *Gordia* isp. because of the complexity of the loops and the ways they are tied together. None of these structures, whether they be trace or body fossils, has much biostratigraphic utility, but they include the only known fossils from the Wyman Formation and are compatible with an Ediacaran age for that unit.

Ichnogenus *Didymaulichnus* Young, 1972

Type ichnospecies. *Fraena lyelli* Rouault, 1850; partim, from Ordovician sandstones of the Armorican Massif of western France, by original designation (Young, 1972).

Didymaulichnus miettensis Young, 1972
Figure 11.1–11.3

Holotype. GSC 27802, ostensibly from the upper part of the Miette Group, but possibly from Cambrian float (Buatois and Mángano, 2016, p. 38), at GSC locality C-5466 near the headwaters of the McGregor River, eastern British Columbia, Canada, by original designation.

Material. LACMIP 43370.3 and LACMIP 43369.20 from the LMWCF, Chicago Pass, California (Fig. 11.1) and Montgomery Mountains, Nevada, plus LACMIP 43373.1, Member IV, Arumbera Formation, Ross River, Northern Territory, Australia (Fig. 11.1).

Remarks. At the type locality, *D. miettensis* is preserved as sandstone casts of bilobed trails that have symmetrically inclined

planar side zones (Young, 1972, fig. 10). That profile is visible in the larger of the two curved traces from the upper part of the LMWCF at Chicago Pass (Fig. 11.1) but the smaller one on the same slab is perhaps more similar to the hypichnial trace (Fig. 11.2) from Member 4 of the Arumbera Formation, central Australia, that was identified by Walter et al. (1989) as *Didymaulichnus lyelli* (Rouault, 1850). Jensen et al. (2002, fig. 5A) illustrated several specimens of *D. miettensis* on the base of a thick sandstone bed from near the top of the LMWCF in section 7333 (Fig. 1.2).

Ichnogenus *Gordia* Emmons, 1844

Type ichnospecies. *Gordia marina* Emmons, 1844, from an Ordovician 'fine flagging stone' (calcareous turbidite) of the Giddings Brook slice, Taconic Allochthon (Landing, 2012), at Mr. M'Arthur's quarry, Jackson, New York, by monotypy.

Gordia isp.
Figures 9.4, 11.4, 11.6

Material. LACMIP 43372.1 (Fig. 9.4), LACMIP 43369.20 (Fig. 11.4), and LACMIP 43372.4 (Fig. 11.6), all from the LMWCF, Montgomery Mountains, Nevada.

Remarks. Specimens from near the top of the LMWCF in section 7333 (Fig. 11.4) and as float in section 7334 (Fig. 9.4) are illustrated, but *Gordia* isp. was also found in situ below the third dolostone in that section (Supplemental dataset 1). The complexity of the loops, with apparent self-level crossing, is the only feature that unites these three examples, so this is a poorly characterized form taxon at this stage. The specimens in Figure 11.4 have a poorly preserved bilobed base, which aligns them with *Didymaulichnus*, but the strongly concentrated circling is unlike the behavior recorded by that ichnogenus.

Ichnogenus *Psammichnites* Torell, 1870

Type ichnospecies. *Psammichnites gigas* (Torell, 1868) from the early Cambrian Hardeberga Formation, Scania, Sweden, by subsequent designation (Fischer and Paulus, 1969).

Remarks. Mángano et al. (2022) subsumed three widely recognized Cambrian ichnospecies, *Psammichnites gigas* (Torell, 1868), *Plagiogmus arcuatus* Roedel, 1929, and *Taphrhelminthopsis circularis* Crimes et al., 1977, into three subspecies of *Psammichnites gigas*: *P. gigas gigas*, *P. gigas circularis*, and *P. gigas arcuatus*. This unusual procedure was carried out for sound paleobiological reasons, but it had the unfortunate consequence of the replacement of a useful keyword 'Plagiogmus' with the cumbersome trinomial term, *Psammichnites gigas arcuatus*. *Psammichnites gigas circularis* and *P. gigas arcuatus* differ from the type subspecies, *P. gigas gigas*, in having the tendency to form extensive loops or 'scribbles' rather than just a generally unidirectional trace, and *P. gigas circularis* lacks the transverse bars that are so characteristic of *P. gigas arcuatus* (Fig. 12.1; Jaeger and Martinsson, 1980; Walter et al., 1989; McIlroy and Heys, 1997; Mángano et al., 2022). All three subspecies are said to co-occur in Member 4 of the Arumbera Formation, central Australia (Mángano et al., 2022, tables 1–3), based on data presented by Walter et al. (1989) and McIlroy and Heys (1997), although those authors preferred to include all examples from the Arumbera Formation in *Plagiogmus arcuatus*.

Psammichnites gigas circularis (Crimes et al., 1977)
Figure 11.5

Holotype. AMC 1219 from the Cambrian Stage 3 Cayetano Beds of the Cándana Formation, Punta del Cerrón, Asturias, Spain (Crimes et al., 1977, pl. 8c; Mángano et al., 2022, fig. 3) by original designation.

Material. LACMIP 43372.3 from the LMWCF, Montgomery Mountains, Nevada (Fig. 11.5).

Remarks. *Psammichnites gigas gigas* co-occurs with *P. gigas circularis* at the type locality of *P. gigas circularis*, but followed less-curved paths. A hand specimen from near the top of the LMWCF in section 7334 (Fig. 1.2) was identified as 'Taphrhelminthopsis' *circularis* by Jensen et al. (2002, fig. 5B) and a complex bilobed scribbling trace from the younger early Cambrian Poleta Formation in the White-Inyo Mountains region was referred to a new species of *Taphrhelminthopsis*, *T. nelsoni*, by Hagadorn, Schellenberg, and Bottjer (2000); Mángano et al. (2022) recommended synonymizing *T. nelsoni* with *P. gigas circularis*. A small specimen outlining an elegant pince-nez shape (Fig. 11.5) may be another example of *P. gigas circularis*.

Psammichnites gigas arcuatus (Roedel, 1929)
Figure 12

Holotype. Specimen figured by Häntzschel (1962, fig. 168.6) from an early Cambrian, glacial erratic, sandstone block, found in northern Germany, but probably sourced from southern Sweden (Roedel, 1929; Jaeger and Martinsson, 1980), by monotypy.

Material. Specimens previously illustrated by Alpert (1974) and Nelson et al. (2019) from the Esmeralda Member, Deep Spring Formation, California and Nevada (Fig. 12.1–12.3, 12.5) plus a small collection from Member IV, Arumbera Sandstone, Amadeus Basin, Australia (Fig. 12.4); LACMIP 26153.1 (= UCLA 49659 from UCLA locality 6153), LACMIP 26160.1 (= UCLA 49670 from UCLA locality 6160), LACMIP 26153.2 (= UCLA 49571 from UCLA locality 6153), LACMIP 26153.3 (= UCLA 49572 from UCLA locality 6153).

Remarks. Although only short segments of the structures are preserved in the small slabs so far recovered from California and Nevada (Fig. 12.1–12.3, 12.5), they are similar to specimens of *P. gigas arcuatus* from the Arumbera Sandstone (Fig. 12.4; McIlroy and Heys, 1997) and early Cambrian glacial erratics in Sweden (Fig. 12.6; Jaeger and Martinsson, 1980), when viewed from their presumed lower side. The U-turn (shown by an arrow in Fig. 12.5) resembles one at the bottom of a Swedish specimen (Fig. 12.6) and surfaces of the burrows from Mount Dunfee (Fig. 12.1) are similar to those of Cloud and Nelson's (1966) specimen and other examples found subsequently in the White-Inyo Mountains (Fig. 1.2, 1.3). A characteristic feature of *Psammichnites gigas arcuatus* and other subspecies of the ichnogenus is a median furrow on the top surface. The lack of this groove in the Deep Spring material may stem from their preservation in less cohesive sediments, which were retaining interstitial fluid during compaction and deformation. As a result, the median furrow, which McIlroy and Heys (1997) attributed to the collapse of an originally cylindrical burrow, did not develop. A possibly comparable morphology is shown by uncompacted burrows of

Psammichnites gigas preserved in very fine-grained quartz arenite from the early Cambrian Backbone Ranges Formation of the Mackenzie Mountains, Canada. One sizeable block has 2- to 3-cm-wide burrows with variably developed, transverse corrugations on their upper surfaces and inconspicuous median grooves (MacNaughton et al., 2021, fig. 4A).

The first appearance of *P. gigas circularis* is considered to be a defining feature of the Fortunian *Rusophycus avalonensis* Zone of Avalonian Newfoundland (Mángano et al., 2022), but *P. gigas arcuatus* also appears during the early Terraneuvian in central and South Australia (Glaessner, 1969; McIlroy and Heys, 1997) and during the Fortunian in Russia (Mángano et al., 2022). Its Great Basin occurrences could be even older, and they encourage the speculation that there is a closer similarity to *Parapsammichnites pretzeliformis* Buatois et al., 2018, from the latest Ediacaran of Namibia than was accepted when that large, complex, looped, and bilobed ichnofossil was first described.

Mángano et al. (2022) differentiated *Parapsammichnites* from *Psammichnites* because the former followed a more diverse course, has plentiful self-overcrossings, pad-like back-fill structures, and lacks an axial furrow. A larger population of 'Plagiogmus' from the Deep Spring Formation is needed before a more detailed comparison with *Parapsammichnites* can be made. Comparison with the Nama Group material is also made difficult by the contrast in preservation; *Parapsammichnites* is mostly preserved in full relief on sandy bed bases at its only known locality, whereas the Deep Spring 'Plagiogmus' specimens seem to be largely intrastratal. In summary, the Deep Spring 'Plagiogmus' material is best interpreted as deformed and unusually preserved examples of *Psammichnites gigas arcuatus*, but more work is needed to confirm this assessment and to explore possible affinities with *Parapsammichnites*.

Ichnogenus ***Treptichnus*** Miller, 1889

Type ichnospecies. *Treptichnus bifurcus* Miller, 1889, from the Carboniferous, Gzhelian, Mansfield Formation of Indiana (Maples and Archer, 1987), by original designation and monotypy.

Treptichnus pedum (Seilacher, 1955)
Figure 10.2, 10.4, 10.6–10.8

Holotype. Specimen figured by Seilacher (1955, p. 387, fig. 4a) from the early Cambrian Neobulus shale (Khussak Formation), Salt Range, Pakistan (Buatois, 2018).

Material. LACMIP 43372.5 and LACMIP 43369.19 from the LMWCF, Montgomery Mountains, Nevada (Fig. 10.2, 10.4, 10.6) and LACMIP 43370.2 from the LMWCF, Chicago Pass, California (Fig. 10.7).

Remarks. Wilson et al. (2012) described and illustrated great variability in traces attributed to *Treptichnus pedum* from incised valley fillings of the Nomtsas Formation, southern Namibia. Those with outwardly projecting probe marks ('segments'; Fig. 10.2, 10.4, 10.6) are the types most commonly considered characteristic of *T. pedum*, but pathways with more subdued segments are also common in the Nomtsas Formation (Fig. 10.8). Both types of traces are present in the LMWCF (e.g., Fig. 10.4 and 10.7). As discussed elsewhere, recent U–Pb ages from within the stratigraphic range of *T. pedum* in the LMWCF (Nelson et al., 2023) make it clear that these occurrences are not earliest Fortunian in age.

Treptichnus spectrum traces
Figures 9.5–9.8, 10.1, 10.3, 10.5, 10.7, 11.6, 11.7

Material. LACMIP 43369.15, LACMIP 43369.16, LACMIP 43369.17, LACMIP 43369.18, and LACMIP 43372.4 from the LMWCF, Montgomery Mountains, Nevada (Figs. 9.5, 9.6, 10.3, 11.6); LACMIP 43370.1 from the LMWCF Chicago Pass, California (Figs. 9.7, 9.8, 10.5, 11.7); LACMIP 43371.1 from the LMWCF, Desert Range, Nevada (Fig. 10.1).

Remarks. Most of the trace fossils from the LMWCF were collected from float, consequently no samples of populations are available to assess within-population variability. Furthermore, some traces vary significantly along their length (Fig. 9.7, 9.8) or express differently levees produced by motion parallel to the substrate versus probes made at right angles to the sediment–water interface. In order to avoid applying too many names to structures that may have been produced by the activities of a single sort of animal, we refer to these traces as the *Treptichnus* spectrum.

Traces of this kind include a specimen found by RJH (Fig. 9.5) at ~10 m above the *Tulaneia* n. gen. level in the 7333 section (Figs. 1.2, 3; Supplemental dataset 1). It occurs with circular structures of the *Nimbia* kind (Fig. 9.5; Fedonkin, 1980), similar to those previously reported from the Stirling Quartzite (Hagadorn and Waggoner, 2000). Other traces at this end of the spectrum occur higher in the LMWCF in the Montgomery Mountains (Figs. 9.6, 10.3) and in the Desert Range (Fig. 10.1). We identify some as *Treptichnus* isp. cf. *T. pedum* (Seilacher, 1955) in the figure explanations, Appendix 1, and Supplemental dataset 1.

Results and Discussion

Ediacaran–Cambrian transition. The proposal by Nelson et al. (2023) to reduce the age of the Ediacaran–Cambrian boundary by ca. 6 Ma was based on the understanding that the FAD of *Treptichnus pedum* in the correlative Montgomery Mountains and Chicago Pass sections corresponded, at least approximately, to the times of its first appearance at the Cambrian GSSP site in Newfoundland (Gehling et al., 2001; Gougeon et al., 2023), Namibia (Jensen et al., 2000; Linnemann et al., 2019; Darroch et al., 2021; Runnegar et al., 2024), Mexico (Hodgin et al., 2021), South Australia (Jensen et al., 1998), and Norway (Högström et al., 2013), and at similar levels elsewhere. Precise U–Pb ages from the upper half of LMWCF of the Spring Mountains section range from 532.83 ± 0.98 to 531.32 ± 0.66 Ma (Nelson et al., 2023). These ages overlap the earlier of two possible estimates for the Fortunian–Stage 2 boundary (531–532 Ma) in New Brunswick, Canada (Bowyer et al., 2022; Hamilton et al., 2024). If these ages are correct, the null hypothesis should be the FAD of *T. pedum* in the LMWCF is late, not earliest Fortunian in age.

At Hines Ridge (Corsetti and Kauffman, 1994; Smith et al., 2023), Molly Gibson (Smith et al., 2023), and Mount Dunfee (Corsetti and Hagadorn, 2003; Smith et al., 2016), a negative carbon isotope excursion within the Deep Spring Formation has been identified as the BACE, the basal Cambrian negative carbon isotope excursion (also known as 'N' or '1n'), which is well expressed in Siberia (e.g., Bartley et al., 1998; Kouchinsky et al., 2007), and has been proposed as the principal criterion for an auxiliary stratotype section and point (ASSP) for the eon boundary (Topper et al., 2022). The trough (nadir) of this excursion is precisely dated as 539.40 ± 0.23 Ma in Mexico (Hodgin et al., 2021) and, as mentioned previously, it coincides with the

occurrences of 'Plagiogmus' (*Psammichnites gigas arcuatus*) at Hines Ridge (extrapolated from Mollie Gibson; Corsetti and Kaufman, 1994, fig. 2), Mollie Gibson (Fig. 1.3; Smith et al., 2023, fig. 7, MGM), and Mount Dunfee (Oliver, 1990, fig. 3; Oliver and Rowland, 2002; Smith et al., 2016, fig. 1; Nelson and Smith, 2019, fig. 1).

Tracing this negative excursion southward into the Death Valley facies is not straightforward because the section thins appreciably and there are far fewer carbonates. Topper et al. (2022, fig. 17) followed earlier suggestions (Corsetti and Kaufman, 1994; Corsetti and Hagadorn, 2000, 2003; Corsetti et al., 2000) in allocating the nadir to the middle dolostone and attributing falling and rising limbs to the lower and upper dolostones, respectively. However, Nelson and Smith (2023, fig. 1) placed the peak at (or just above?) the top of the first major dolostone in the Boundary Canyon and Montgomery Mountains sections, presumably on the assumption that this is a disconformable surface. In this interpretation, the interval of the LMWCF yielding *Tulaneia amabilia* n. gen. n. sp. and *Saarina hagadorni* Selly et al., 2020, predates the nadir and is latest Ediacaran in age; the remainder of the LMWCF postdates the nadir and is therefore Cambrian in age, for reasons already given. However, in order to reconcile the Spring and Montgomery Mountains sections of the LMWCF, it was necessary for Nelson et al. (2023, fig. 1) to postulate that the lowest dolostone in the Montgomery Mountains preserves only the declining limb of the BACE excursion, whereas the same dolostone in the adjacent (~20 km away) Spring Mountains section records only part of its post-nadir rise.

If this correlation between the White-Inyo and Death Valley facies is correct, then in the Spring Mountains and nearby exposures of the LMWCF, ca. 6.6 Ma of time must be compressed into 30–50 m of stratigraphic section (Nelson et al., 2023, fig. 1). Given the complexity of the Fortunian carbon isotope record in Siberia, with three positive (2p–4p) and three negative (2n–4n) events before the positive excursion (5p) near the Fortunian–Stage 2 boundary (Kouchinsky et al., 2007; Zhuravlev et al., 2023), it is unlikely that any particular named excursion could be recognized in the sparsely sampled and probably incomplete carbon isotope record of the LMWCF. The suggestion (Nelson et al., 2023, fig. 1) that the whole of the Cambrian part of the LMWCF represents merely the 1n to 2p secular increase in $\delta^{13}C$, as seen, for example, in the Sukharihka section of the Siberian platform (Kouchinsky et al., 2007, fig. 2), is unrealistic in light of the U–Pb age constraints. Given these uncertainties, we prefer to defer to lithological and paleontological criteria to correlate the White-Inyo and Death Valley successions, but note that the ca. 539 Ma age for the BACE nadir in Mexico corresponds to the middle (Esmeralda Member) of the Deep Spring Formation in California and Nevada, and that the nadir of the BACE excursion is unlikely to be older than the top of the first major dolostone of the LMWCF, according to traditional lithostratigraphic evidence (Stewart, 1966, 1970). There are also two paleontological matters that are worthy of consideration in this context. First, could *Psammichnites gigas arcuatus* have appeared during the Ediacaran? And second, could *Tulaneia amabilia* n. gen. n. sp. be Cambrian in age?

Mángano et al. (2022) noted that the first appearance of *Psammichnites gigas circularis* is one of the diagnostic elements of the [early Fortunian] *Rusophycus avalonensis* Zone. *Psammichnites gigas arcuatus*, which only differs from *P. gigas circularis* in having the ladder-like burrow base (Fig. 12.1), occurs in the Fortunian of Siberia (Mángano et al., 2022, table 3) and

possibly in the earliest Fortunian (parasequence 3 of the Ingta Formation) in Canada (Carbone and Narbonne, 2014, fig. 4.1). An allied ichnofossil, *Parapsammichites pretzeliformis*, has been found in the undisputedly Ediacaran part of the Spitskop Member of the Schwarzrand Subgroup of Namibia (Buatois et al., 2018), so this degree of behavioral complexity began well before the Cambrian. Thus, we cannot rule out an Ediacaran age for the Deep Spring Formation 'Plagiogmus', but the default hypothesis must be that it is Cambrian or younger until proven otherwise.

There are also suggestions that some erniettomorphs may have survived into the Cambrian (Jensen et al., 1998; Hagadorn et al., 2000; Hoyal Cuthill, 2022; Mussini and Dunn, 2024; but see Runnegar et al., 2024), but if *Tulaneia amabilia* n. gen. n. sp. is restricted to the interval below the first major dolostone of the LMWCF, as seems likely, the nature of the associated body and trace fossils makes an earliest Cambrian age both implausible and unnecessary. In summary, all available evidence suggests that *Tulaneia amabilia* n. gen. n. sp. is latest Ediacaran in age, the Ediacaran–Cambrian boundary in the Death Valley succession coincides with the top of the first major dolostone of the LMWCF, and that the remainder of the LMWCF spans most of the early Cambrian Fortunian Stage.

Great Unconformity. Peters and Gaines (2012) showcased the 'Great Unconformity' at the base of the Sauk megasequence as a possible trigger for the Cambrian explosion. They noted that the base of the Sauk is diachronous (Sloss, 1963, 1988), but argued that it is a unique, globally occurring stratigraphic surface that, through unprecedented chemical weathering and erosion, may have modified ocean water chemistry enough to have influenced the evolution of biomineralization. The basis for this hypothesis was reviewed by Shahkarami et al. (2020), who concluded that the unconformable 'surface' has multiple local origins and should not be used for global correlation. We mention the hypothesis here because of the new, late Fortunian age, for the top of the LMWCF and, therefore, the base of the Sauk megasequence at the craton margin, which was well separated in time from the Ediacaran–Cambrian boundary in this area.

Erniettomorphs. Because it has long been confused with *Ernietta*, there seems little doubt that *Tulaneia amabilia* n. gen. n. sp. is an erniettomorph, as defined in Runnegar et al. (2024). Diagnostic features are all related to the modular, tubular construction, seen also in *Ernietta* (Ivantsov et al., 2016), *Pteridinium* (Elliott et al., 2016; Darroch et al., 2022; Runnegar et al., 2024), and *Phyllozoon* (Gehling and Runnegar, 2022), each of which is readily distinguished by its unique geometry. Unfortunately, the addition of *Tulaneia* n. gen. to the clade provides little enlightenment as to the nature of their bodies, their modes of life, or their place in the tree of life. Our best guess is that *Tulaneia* n. gen. housed facultative or obligate bacterial symbionts that used sunlight and/or reduced compounds plus oxygen to grow, reproduce, and to supply nutrients to the host organism. We speculate that *Tulaneia* n. gen. was epifaunal, attached somehow at its basal seam, and inhabited nearshore sandy bottoms well within the photic zone. As to its place in the tree of life, the simplicity of its morphology, even when compared with *Ernietta*, may indicate a position lower in the metazoan tree than the crown group, if these organisms are indeed metazoans.

References

Ahn, S.Y., Babcock, L.E., and Hollingsworth, J.S., 2012, Revised stratigraphic nomenclature for parts of the Ediacaran–Cambrian Series 2 succession in the southern Great Basin, USA: *Memoirs of the Association of Australasian Palaeontologists*, v. **42**, p. 105–114.

Alpert, S.P., 1974, *Trace Fossils of the Precambrian–Cambrian Succession, White-Inyo Mountains, California*: Los Angeles, University of California, Los Angeles, 162 p.

Alpert, S.P., 1975, *Planolites* and *Skolithos* from the upper Precambrian–lower Cambrian White-Inyo Mountains, California: *Journal of Paleontology*, v. **49**, p. 508–521.

Alpert, S.P., 1976, Trilobite and star-like trace fossils from the White-Inyo Mountains, California: *Journal of Paleontology*, v. **50**, p. 226–239.

Bartley, J.K., Pope, M., Knoll, A.H., Semikhatov, M.A., and Petrov, P.Yu., 1998, A Vendian–Cambrian boundary succession from the northwestern margin of the Siberian Platform: stratigraphy, palaeontology, chemostratigraphy and correlation: *Geological Magazine*, v. **135**, p. 473–494.

Bergmann, K.D., Zentmyer, R.A., and Fischer, W.W., 2011, The stratigraphic expression of a large negative carbon isotope excursion from the Ediacaran Johnnie Formation, Death Valley: *Precambrian Research*, v. **188**, p. 45–56.

Bobrovskiy, I., Nagovitsyn, A., Hope, J.M., Luzhnaya, E., and Brocks, J.J., 2022, Guts, gut contents, and feeding strategies of Ediacaran animals: *Current Biology*, v. **32**, p. 5382–5389.e3, https://doi.org/10.1016/j.cub.2022.10.051.

Bowyer, F.T., Zhuravlev, A.Yu., Wood, R., Shields, G.A., et al., 2022, Calibrating the temporal and spatial dynamics of the Ediacaran–Cambrian radiation of animals: *Earth-Science Reviews*, v. **225**, 103913, https://doi.org/10.1016/j.earscirev.2021.103913.

Bowyer, F.T., Zhuravlev, A.Y., Wood, R., Zhao, F., Sukhov, S.S., Alexander, R.D., Poulton, S.W., and Zhu, M., 2023, Implications of an integrated late Ediacaran to early Cambrian stratigraphy of the Siberian Platform, Russia: *GSA Bulletin*, v. **135**, p. 2428–2450.

Buatois, L.A., 2018, *Treptichnus pedum* and the Ediacaran–Cambrian boundary: significance and caveats: *Geological Magazine*, v. **155**, p. 175–180.

Buatois, L.A., and Mángano, M.G., eds., 2016, The Trace-Fossil Record of Major Evolutionary Events. Volume 1: *Precambrian and Paleozoic*: Berlin, Springer, 358 p.

Buatois, L.A., Almond, J., Mángano, M.G., Jensen, S., and Germs, G.J.B., 2018, Sediment disturbance by Ediacaran bulldozers and the roots of the Cambrian explosion: *Scientific Reports*, v. **8**, 4514, https://doi.org/10.1038/s41598-018-22859-9.

Budd, G.E., and Jackson, I.S.C., 2015, Ecological innovations in the Cambrian and the origins of the crown group phyla: *Philosophical Transactions of the Royal Society B*, v. **371**, 20150287, https://doi.org/10.1098/rstb.2015.0287.

Carbone, C.A., and Narbonne, G.M., 2014, When life got smart: the evolution of behavioral complexity through the Ediacaran and early Cambrian of NW Canada: *Journal of Paleontology*, v. **88**, p. 309–330.

Chai, S., Wu, Y., and Hua, H., 2021, Potential index fossils for the terminal stage of the Ediacaran System: *Journal of Asian Earth Sciences*, v. **218**, 104885, https://doi.org/10.1016/j.jseaes.2021.104885.

Cloud, P.E., and Bever, J.E., 1973, Trace fossils from the Flathead Sandstone, Fremont County, Wyoming, compared with early Cambrian forms from California and Australia: *Journal of Paleontology*, v. **47**, p. 883–885.

Cloud, P.E., and Nelson, C.A., 1966, Phanerozoic–Cryptozoic and related transitions: new evidence: *Science*, v. **154**, p. 766–770.

Cloud, P.E., and Nelson, C.A., 1967, *Pteridinium* and the Precambrian–Cambrian boundary: *Science*, v. **157**, p. 957–958.

Corsetti, F.A., and Hagadorn, J.W., 2000, Precambrian–Cambrian transition: Death Valley, United States: *Geology*, v. **28**, p. 299–302.

Corsetti, F.A., and Hagadorn, J.W., 2003, The Precambrian–Cambrian transition in the southeastern Great Basin: *The Sedimentary Record*, v. **1**, p. 4–8.

Corsetti, F.A., and Kauffman, A.J., 1994, Chemostratigraphy of Neoproterozoic–Cambrian units, White-Inyo region, eastern California and western Nevada: implications for global correlation and faunal distribution: *Palaios*, v. **9**, p. 211–219.

Corsetti, F.A., Awramik, S.M., Pierce, D., and Kaufman, A.J., 2000, Using chemostratigraphy to correlate and calibrate unconformities in Neoproterozoic strata from the southern Great Basin of the United States: *International Geology Review*, v. **42**, p. 516–533.

Crimes, T.P., Legg, I., Marcos, A., and Arboleya, M., 1977, ?Late Precambrian–low lower Cambrian trace fossils from Spain, *in* Crimes, T.P., and Harper, J.C., eds., *Trace Fossils 2*: Geological Journal Special Issue, v. **9**, p. 91–138.

Darroch, S.A.F., Smith, E.F., Laflamme, M., and Erwin, D.H., 2018, Ediacaran extinction and Cambrian explosion: *Trends in Ecology and Evolution*, v. **33**, p. 653–663.

Darroch, S.A.F., Cribb, A.T., Buatois, L.A., Germs, G.J.B., Kenchington, C.G., et al., 2021, The trace fossil record of the Nama Group, Namibia: exploring the terminal Ediacaran roots of the Cambrian explosion: *Earth-Science Reviews*, v. **212**, 103435, https://doi.org/10.1016/j.earscirev.2020.103435.

Darroch, S.A.F., Gibson, B.M., Syversen, M., Rahman, I.A., Racicot, R.A., Dunn, F.S., Gutarra, S., Schindler, E., Wehrmann, A., and Laflamme, M., 2022, The life and times of *Pteridinium simplex*: *Paleobiology*, v. **48**, p. 527–556.

Diehl, P., 1976, Stratigraphy and sedimentology of the Wood Canyon Formation, Death Valley area, California: *California Division of Mines and Energy Special Report*, v. **106**, p. 51–62.

Durham, J.W., 1974, On the Precambrian–early Cambrian trace fossil *Plagiogmus*: *Geological Society of America Abstracts with Programs*, v. **6**, n. 3, p. 170.

Elliott, D.A., Trusler, P.W., Narbonne, G.M., Vickers-Rich, P., Morton, N., Hall, M., Hoffmann, K.H., and Schneider, G.I.C., 2016, *Ernietta* from the late Ediacaran Nama Group, Namibia: *Journal of Paleontology*, v. **90**, p. 1017–1026.

Emmons, E., 1844, *The Taconic System; Based on Observations in New York, Massachusetts, Maine, Vermont and Rhode-Island*: Albany, Carroll and Cook, 68 p.

Fedo, C.M., and Cooper, J.D., 1990, Braided fluvial to marine transition: the basal lower Cambrian Wood Canyon Formation, southern Marble Mountains, Mojave Desert, California: *Journal of Sedimentary Petrology*, v. **60**, p. 220–234.

Fedo, C.M., and Cooper, J.D., 2001, Sedimentology and sequence stratigraphy of Neoproterozoic and Cambrian units across a craton–margin hinge zone, southeastern California, and implications for the early evolution of the Cordilleran margin: *Sedimentary Geology*, v. **141–142**, p. 501–522.

Fedonkin, M.A., 1980, (Fossil traces of Precambrian Metazoa): *Izvestiya of the Academy of Sciences of the U.S.S.R., Geological Series*, v. **1**, p. 39–46. [in Russian]

Fischer, P., and Paulus, B., 1969, Spurenfossilien aus den Oberen Nohn-Schichten der Blankenheimer Mulde (Eifelium, Eifel): *Senckenbergiana Lethaea*, v. **50**, p. 81–101.

Gallick, C.M., 1964, *The geology of part of the Blanco Mountain Quadrangle, Inyo County, California [M.A. thesis]*: Los Angeles, University of California, Los Angeles, 100 p.

Gehling, J.G., and Runnegar, B., 2022, *Phyllozoon* and *Aulozoon*: key components of a novel Ediacaran death assemblage in Bathtub Gorge, Heysen Range, South Australia: *Geological Magazine*, v. 159, p. 1134–1147.

Gehling, J.G., Jensen, S., Droser, M.L., Myrow, P.M., and Narbonne, G.M., 2001, Burrowing below the basal Cambrian GSSP, Fortune Head, Newfoundland: *Geological Magazine*, v. 138, p. 213–218.

Gillett, S.L., and Van Alstine, D.R., 1979, Paleomagnetism of lower and middle Cambrian sedimentary rocks from the Desert Range, Nevada: *Journal of Geophysical Research Solid Earth*, v. 84, p. 4475–4489.

Glaessner, M.F., 1969, Trace fossils from the Precambrian and basal Cambrian: *Lethaia*, v. 2, p. 369–393.

Gougeon, R., Mángano, M.G., Buatois, L.A., Narbonne, G.M., Laing, B.A., and Paza, M., 2023, The Ediacaran–Cambrian Chapel Island Formation of Newfoundland, Canada: evaluating the impact of outcrop quality on trace-fossil data sets at the Cambrian GSSP and less-explored sections: *Canadian Journal of Earth Sciences*, v. 60, p. 897–911.

Hagadorn, J.W., and Waggoner, B.M., 2000, Ediacaran fossils from the southwestern Great Basin, United States: *Journal of Paleontology*, v. 74, p. 349–359.

Hagadorn, J.W., Schellenberg, S.A., and Bottjer, D.J., 2000, Paleoecology of a large early Cambrian bioturbator: *Lethaia*, v. 33, p. 142–156.

Hall, J.G., Smith, E.F., Tamura, N., Fakra, S.C., and Bosak, T., 2020, Preservation of erniettomorph fossils in clay-rich siliciclastic deposits from the Ediacaran Wood Canyon Formation, Nevada: *Interface Focus*, v. 10, 20200012, https://doi.org/10.1098/rsfs.2020.0012.

Hamilton, M.A., Álvaro, J.J, Barr, S.M., Jensen, S., Johnson, S.C., Palacios, T., van Rooyen, D., and White, C.E., 2024, U–Pb zircon ages from tuffaceous beds in the Terreneuvian to Cambrian Series 2 sections of Avalonian southern New Brunswick, Canada: new constraints on chronostratigraphic correlations and the Cambrian time scale: *Geological Society, London, Special Publications*, v. 542, p. 217–237.

Häntzschel, W., 1962, Trace fossils and problematica, *in* Moore, R.C., ed., *Treatise on Invertebrate Paleontology W*: Lawrence, Kansas, Geological Society of America and University of Kansas Press, p. W177–W245.

Hodgin, E.B., Nelson, L.L., Wall, C.J., Barrón-Díaz, A.J., Webb, L.C., Schmitz, M.D., Fike, D.A., Hagadorn, J.W., and Smith, E.F., 2021, A link between rift-related volcanism and end-Ediacaran extinction? Integrated chemostratigraphy, biostratigraphy, and U–Pb geochronology from Sonora, Mexico: *Geology*, v. 49, p. 115–119.

Hogan, E.G., Fedo, C.M., and Cooper, J.D., 2011, Reassessment of the basal Sauk supersequence boundary across the Laurentian craton–margin hinge zone, southeastern California: *Journal of Geology*, v. 119, p. 661–685.

Högström, A.E.S., Jensen, S., Palacios, T., and Ebbestad, J.O.R., 2013, New information on the Ediacaran–Cambrian transition in the Vestertana Group, Finnmark, northern Norway, from trace fossils and organic-walled microfossils: *Norwegian Journal of Geology*, v. 93, p. 95–106.

Hollingsworth, J.S., 2011, Lithostratigraphy and biostratigraphy of Cambrian Stage 3 in western Nevada and eastern California, in Hollingsworth, J.S., Sundberg, F.A., and Foster, J.R., eds., *Cambrian Stratigraphy and Paleontology of Northern Arizona and Southern Nevada. The 16th Field Conference of the Cambrian Stage Subdivision Working Group International Subcommission on Cambrian Stratigraphy Flagstaff, Arizona, and Southern Nevada, United States*: Museum of Northern Arizona Bulletin, v. 67, p. 26–42.

Horodyski, R.J., 1991, Late Proterozoic megafossils from southern Nevada: *Geological Society of America Abstracts with Programs*, v. 23, n. 6, p. A163.

Horodyski, R.J., Gehling, J.G., Jensen, S., and Runnegar, B., 1994, Ediacaran fauna and earliest Cambrian trace fossils in a single parasequence set, southern Nevada: *Geological Society of America Abstracts with Programs*, v. 26, n. 2, p. 60.

Hoyal Cuthill, J.F., 2022, Ediacaran survivors in the Cambrian: suspicions, denials and a smoking gun: *Geological Magazine*, v. 159, p. 1210–1219.

Ivantsov, A.Yu., Narbonne, G.M., Trusler, P.W., Greentree, C., and Vickers-Rich, P., 2016, Elucidating *Ernietta*: new insights from exceptional specimens in the Ediacaran of Namibia: *Lethaia*, v. 49, p. 540–554.

Jaeger, H., and Martinsson, A., 1980, The early Cambrian trace fossil *Plagiogmus* in its type area: *Geologiska Föreningens i Stockholm Förhandlingar*, v. 102, p. 117–126.

Jenkins, R.J.F., Plummer, P.S., and Moriarty, K.C., 1981, Late Precambrian pseudofossils from the Flinders Ranges, South Australia: *Transactions of the Royal Society of South Australia*, v. 105, p. 67–83.

Jensen, S., and Grant, S.W., 1996, Chemostratigraphy of Neoproterozoic–Cambrian units, White-Inyo region, eastern California and western Nevada: implications for global correlation and faunal distribution: *Comment: Palaios*, v. 11, p. 83–86.

Jensen, S., Gehling, J.G., and Droser, M.L., 1998, Ediacara-type fossils in Cambrian sediments: *Nature*, v. 393, p. 567–569.

Jensen, S., Saylor, B.Z., Gehling, J.G., and Germs, G.J.B., 2000, Complex trace fossils from the terminal Proterozoic of Namibia: *Geology*, v. 28, p. 143–146.

Jensen, S., Droser, M.L., and Heim, A.E., 2002, Trace fossils and ichnofabrics of the lower Cambrian Wood Canyon Formation, southwest Death Valley area, *in* Corsetti, F.A., ed., *Proterozoic–Cambrian of the Great Basin and Beyond*: Pacific Section SEPM Fieldtrip Guidebook 93, p. 123–135.

Jensen, S., Droser, M.L., and Gehling, J.G., 2006, A critical look at the Ediacaran trace fossil record, *in* Xiao, S., and Kaufman, A.J., eds, *Neoproterozoic Geobiology and Paleobiology*: Berlin, Springer, p. 115–157.

Kaufman, A.J., and Corsetti, F.A., 1996, Chemostratigraphy of Neoproterozoic–Cambrian units, White-Inyo region, eastern California and western Nevada: implications for global correlation and faunal distribution: Reply: *Palaios*, v. 11, p. 86–89.

Keller, M., Lehnert, O., and Cooper, J.D., 2012, Sauk megasequence supersequences, southern Great Basin: second-order accommodation events on the southwestern Cordilleran margin platform, *in* Derby, J., Fritz, R., Longacre, S., Morgan, W., and Sternbach, C., eds., *Great American Carbonate Bank: the Geology and Economic Resources of the Cambrian–Ordovician Sauk Megasequence of Laurentia*: American Association of Petroleum Geologists Memoir, v. 98, p. 873–896.

Kouchinsky, A., Bengtson, S., Pavlov, V., Runnegar, B., Torssander, P., Young, E., and Ziegler, K., 2007, Carbon isotope stratigraphy of the Precambrian–Cambrian Sukharikha River section, northwestern Siberian platform: *Geological Magazine*, v. 144, p. 609–618.

Landing, E., 2012, The great American carbonate bank in eastern Laurentia: its births, deaths, and linkage to paleooceanic oxygenation (early Cambrian–Late Ordovician), *in* Derby, J., Fritz, R., Longacre, S., Morgan, W., and Sternbach, C., eds., *Great American Carbonate Bank: the Geology and Economic Resources of the Cambrian–Ordovician Sauk Megasequence of Laurentia*: American Association of Petroleum Geologists Memoir, v. 98, p. 451–492.

Langille, G.B., 1973, "Uppermost Precambrian–lowermost Cambrian" ichnocoenoses, Inyo County, California: *Geological Society of America Abstracts with Programs*, v. 5, n. 2, p. 186.

Langille, G.B., 1974, Earliest Cambrian–latest Proterozoic ichnofossils and problematic fossils from Inyo County, California [Ph.D. dissertation]: Binghamton, New York, State University of New York, Binghamton, 194 p.

Linnemann, U., Ovtcharova, M., Schaltegger, U., Gärtner, A., Hautmann, M., et al., 2019, New high-resolution age data from the Ediacaran–Cambrian boundary indicate rapid, ecologically driven onset of the Cambrian explosion: *Terra Nova*, v. 31, p. 49–58.

MacNaughton, R.B., Fallas, K.M., and Finley, T.D., 2021, *Psammichnites gigas* from the lower Cambrian of the Mackenzie Mountains, northwest Canada, and their biostratigraphic implications: *Ichnos*, v. 28, p. 164–175.

Mángano, M.G., Buatois, L.A., MacNaughton, R.B., Jensen, S., Gougeon, R., Marcos, A., Meek, D., Piñuela, L., and García-Ramos, J.C., 2022, The *Psammichnites–Taphrhelminthopsis* conundrum: implications for calibrating the Cambrian explosion: *Earth Science Reviews*, v. 227, 103971, https://doi.org/10.1016/j.earscirev.2022.103971.

Maples, C.G., and Archer, A.W., 1987, Redescription of Early Pennsylvanian trace-fossil holotypes from the nonmarine Hindostan Whetstone Beds of Indiana: *Journal of Paleontology*, v. 61, p. 890–897.

McIlroy, D., and Heys, G.R., 1997, Palaeobiological significance of *Plagiogmus arcuatus* from the lower Cambrian of central Australia: *Alcheringa*, v. 21, p. 161–178.

McMenamin, M.A.S., 1998, *The Garden of Ediacara: Discovering the First Complex Life*: New York, Columbia University Press, 295 p.

Miller, S.A., 1889, *North American Geology and Paleontology for the Use of Amateurs, Students and Scientists*: Cincinnati, Ohio, Western Methodist Book Concern, 664 p.

Muhlbauer, J.G., Fedo, C.M., and Moersch, J.E., 2020, Architecture of a distal pre-vegetation braidplain: Cambrian middle member of the Wood

Canyon Formation, southern Marble Mountains, California, USA: *Sedimentology*, v. **67**, p. 1084–1113.

Mussini, G., and Dunn, F.S., 2024, Decline and fall of the Ediacarans: late-Neoproterozoic extinctions and the rise of the modern biosphere: *Biological Reviews*, v. **99**, p. 110–130.

Narbonne, G.M., Saylor, B.Z., and Grotzinger, J.P., 1997, The youngest Ediacaran fossils from southern Africa: *Journal of Paleontology*, v. **71**, p. 953–967.

Nelson, C.A., 1966, *U.S.* Geological Survey Geologic Quadrangle Map, Blanco Mountain, GQ-529.

Nelson, C.A., 1978, Late Precambrian–early Cambrian stratigraphic and faunal succession of eastern California and the Precambrian–Cambrian boundary: *Geological Magazine*, v. **115**, p. 121–126.

Nelson, L.L., and Smith, E.F., 2019, Tubey or not tubey: death beds of Ediacaran macrofossils or microbially induced sedimentary structures?: *Geology*, v. **47**, p. 909–913.

Nelson, L.L., and Smith, E.F., 2020, Tubey or not tubey: death beds of Ediacaran macrofossils or microbially induced sedimentary structures?: Reply: *Geology*, v. **48**, p. e498, https://doi.org/10.1130/G47059Y.1.

Nelson, L.L., Crowley, J.L., Smith, E.F., Schwartz, D.M., Hodgin, E.B., and Schmitz, M.D., 2023, Cambrian explosion condensed: high-precision geochronology of the lower Wood Canyon Formation, Nevada: *Proceedings of the National Academy of Sciences U.S.A.*, v. **120**, e2301478120, https://doi.org/10.1073/pnas.2301478120.

Noffke, N., 2009, The criteria for the biogeneicity of microbially induced sedimentary structures (MISS) in Archean and younger, sandy deposits: *Earth-Science Reviews*, v. **96**, p. 173–180.

Oliver, L., 1990, *Stromatolites of the lower Cambrian Deep Spring Formation; Mount Dunfee, Esmeralda County, Nevada [M.S. thesis]*: Las Vegas, University of Nevada, Las Vegas, 150 p.

Oliver, L. K., and Rowland, S. M., 2002. Microbialite reefs at the close of the Proterozoic eon: the Middle Member Deep Spring Formation at Mt. Dunfee, Nevada, *in* Corsetti, F.A., ed., *Proterozoic–Cambrian of the Great Basin and Beyond*: Pacific Section SEPM Fieldtrip Guidebook 93, p. 97–122.

O'Neil, G.R., Tackett, L.S., and Meyer, M.B., 2022, The role of surficial bioturbation in the latest Ediacaran: a quantitative analysis of trace fossil intensity in the terminal Ediacaran–lower Cambrian of California: *Palaios*, v. **37**, p. 703–717.

Peters, S.E., and Gaines, R.R., 2012, Formation of the 'Great Unconformity' as a trigger for the Cambrian explosion: *Nature*, v. **484**, p. 363–366.

Pflug, H.D., 1966, Neue Fossilreste aus den Nama-Schichten in Südwest-Africa: *Paläontologische Zeitschrift*, v. **40**, p. 14–25.

Pflug, H.D., 1972, Zur Fauna der Nama-Schichten in Südwest-Afrika III. Erniettomorpha, Bau und Systematik: *Palaeontographica Abt. A*, v. **139**, p. 134–170.

Prave, A.R., Fedo, C.M., and Cooper, J.D., 1991, Lower Cambrian depositional and sequence stratigraphic framework of the Death Valley and eastern Mojave regions, *in* Walawender, M.J., and Hanan, B.B., eds., *Geological Excursions in Southern California and Mexico*: San Diego, California, Department of Geological Sciences, San Diego State University, p. 147–170.

Roedel, H., 1929, Ergänzung zu meiner Mitteilung über ein kambrisches Geschiebe mit problematischen Spuren: *Zeitschrift fiir Geschiebeforschung*, v. **5**, p. 48–51.

Rouault, M., 1850, Note préliminaire sur une nouvelle formation découverte dans le terrain Silurien inférieur de la Bretagne: *Société Géologique de France Bulletin, ser. 2*, v. **7**, p. 724–744.

Runnegar, B., 1998, Precambrian–Cambrian boundary in the southern Great Basin, California and Nevada, and the base of the Sauk sequence: *Geological Society of America Annual Meeting Abstracts with Programs*, v. **30**, p. 63.

Runnegar, B., 2022, Following the logic behind biological interpretations of the Ediacaran biotas: *Geological Magazine*, v. **159**, 1093–1117.

Runnegar, B., and Fedonkin, M.A., 1992, Proterozoic metazoan body fossils, *in* Schopf, J.W. and Klein, C., eds., *The Proterozoic Biosphere, A Multidisciplinary Study*: Cambridge, UK, Cambridge University Press, p. 369–388.

Runnegar, B., Gehling, J.G., Jensen, S., and Saltzman, M.R., 2024, Ediacaran paleobiology and biostratigraphy of the Nama Group, Namibia, with emphasis on the erniettomorphs, tubular and trace fossils, and a new sponge, *Arimasia germsi* n. gen. n. sp.: *Journal of Paleontology*, v. **98**, suppl. 94, 59 p.

St. Jean, J., 1973, A new Cambrian trilobite from the Piedmont of North Carolina: *American Journal of Science*, v. **273A**, p. 196–216.

Schiffbauer, J.D., Huntley, J.W., O'Neil, G.R., Darroch, S.A.F., Laflamme, M., and Cai, Y., 2016, The latest Ediacaran wormworld fauna: setting the ecological stage for the Cambrian Explosion: *GSA Today*, v. **26**, n. 11, p. 4–11.

Seilacher, A. 1955. Spuren und fazies im Unterkambrium, *in* Schindewolf, O.H., and Seilacher, A., eds., *Beitrage zur Kenntnis des Kambriums in der Salt Range*: Abhandlungen Akademie der Wissenschaften und der Literatur zu Mainz, Mathematisch-Naturwissenschaftliche Klasse, v. **10**, p. 373–399.

Selly, T., Schiffbauerb, J.D., Jacquet, S.M., Smith, E.F., Nelson, L.L., *et al.*, 2020, A new cloudinid fossil assemblage from the terminal Ediacaran of Nevada, USA: *Journal of Systematic Palaeontology*, v. **18**, p. 357–379.

Shahkarami, S., Buatois, L.A., Mángano, M.G., and Hagadorn, J.W., 2020, The Ediacaran–Cambrian boundary: evaluating stratigraphic completeness and the Great Unconformity: *Precambrian Research*, v. **345**, 105721, https://doi.org/10.1016/j.precamres.2020.105721.

Signor, P.W., Mount, J.F., and Onken, B.R., 1987, A pre-trilobite shelly fauna from the White-Inyo region of eastern California and western Nevada: *Journal of Paleontology*, v. **61**, p. 425–438.

Sloss, L.L., 1963, Sequences in the cratonic interior of North America: *Geological Society of America Bulletin*, v. **74**, p. 93–114.

Sloss, L.L., 1988, Forty years of sequence stratigraphy: *Geological Society of America Bulletin*, v. **100**, p. 1661–1665.

Smith, E.F., Nelson, L.L., Strange, M.A., Eyster, A.E., Rowland, S.M., Schrag, D.P., and Macdonald, F.A., 2016, The end of the Ediacaran: two exceptionally preserved body fossil assemblages from Mt. Dunfee, Nevada: *Geology*, v. **44**, p. 911–914.

Smith, E.F., Nelson, L.L., Tweedt, S.M., Zeng, H., and Workman, J.B., 2017, A cosmopolitan late Ediacaran biotic assemblage: new fossils from Nevada and Namibia support a global biostratigraphic link: *Proceedings of the Royal Society B*, v. **284**, 20170934, https://doi.org/10.1098/rspb.2017.0934.

Smith, E.F., Nelson, L.L., O'Connell, N., Eyster, A., and Lonsdale, M.C., 2023, The Ediacaran–Cambrian transition in the southern Great Basin, United States: *Geological Society of America Bulletin*, v. **135**, p. 1393–1414.

Stewart, J.H., 1966, Correlation of lower Cambrian and some Precambrian strata in the southern Great Basin, California and Nevada: *United States Geological Survey Professional Paper*, v. **550-C**, p. 66–72.

Stewart, J.H., 1970, Upper Precambrian and lower Cambrian strata in the southern Great Basin, California and Nevada: *United States Geological Survey Professional Paper*, v. **620**, p. 1–206.

Tarhan, L.G., Myrow, P.M., Smith, E.F., Nelson, L.L., and Sadler, P.M., 2020, Infaunal augurs of the Cambrian explosion: an Ediacaran trace fossil assemblage from Nevada, USA: *Geobiology*, v. **18**, p. 486–496.

Topper, T., Betts, M.J., Dorjnamjaa, D., Li, G., Li, L., Altanshagai, G., Enkhbaatar, B., and Skovsted, C.B., 2022, Locating the BACE of the Cambrian: Bayan Gol in southwestern Mongolia and global correlation of the Ediacaran–Cambrian boundary: *Earth-Science Reviews*, v. **229**, 104017, https://doi.org/10.1016/j.earscirev.2022.104017.

Torell, O.M., 1868, Bidrag till Sparagmitetagens geognosti och paleontology: *Acta Universitatis Lundensis. Lunds Universitets Års-skrift*, v. **2**, p. 1–40.

Torell, O.M., 1870, Petrificata Suecana Formationis Cambricae: *Acta Universitatis Lundensis. Lunds Universitets Års-skrift*, v. **6**, p. 1–14.

Walter, M.R., Elphinstone, R., and Heys, G.R., 1989, Proterozoic and early Cambrian trace fossils from the Amadeus and Georgina basins, central Australia: *Alcheringa*, v. **13**, p. 209–256.

Wilson, J.P., Grotzinger, J.P., Fischer, W.W., Hand, K.P., Jensen, S., *et al.*, 2012, Deep-water incised valley deposits at the Ediacaran–Cambrian boundary in southern Namibia contain abundant *Treptichnus pedum*: *Palaios*, v. **27**, p. 252–273.

Young, F.G, 1972. Early Cambrian and older trace fossils from the southern Cordillera of Canada: *Canadian Journal of Earth Sciences*, v. **9**, p. 1–17.

Zhuravlev, A.Yu., Wood, R., and Bowyer, F.T., 2023, Cambrian radiation speciation events driven by sea level and redoxcline changes on the Siberian Craton: *Science Advances*, v. **9**, eadh2558, https://doi.org/10.1126/sciadv.adh2558.

Appendix 1: descriptions of fossil localities used for this study

Mollie Gibson, Inyo County, California

UCLA 6153/LACMIP 26153 (Fig. 1.3; Alpert, 1974).—Esmeralda Member, Deep Spring Formation at intersection of mining road and stream bed, ~230 m E and ~190 m N of SW corner sec. 15, T7S, R35E, ~1.4 km SE of the Mollie Gibson mines (37.344538°N, 118.142230°W), Blanco Mountain Quadrangle, California; Cambrian (Fortunian).

    Psammichnites gigas arcuatus (Roedel, 1929) (Fig. 12.2; Alpert, 1974, pl. 5, figs 3, 11, 12).

UCLA 6160/LACMIP 26160 (Fig. 1.3; locality 6 of Cloud and Nelson, 1966, fig. 3; Alpert, 1974).—Esmeralda Member, Deep Spring Formation, NE¼, NW¼, SE¼, sec. 16, T7S, R35E, ~600 m SE of Mollie Gibson mines (37.344538°N, 118.142230°W), Blanco Mountain Quadrangle, California; Cambrian (Fortunian).

    Psammichnites gigas arcuatus (Roedel, 1929) (Fig. 12.2 right, 12.3; Cloud and Nelson, 1966, fig. 1B; Cloud and Bever, 1973, pl. 1, fig. 5; Alpert, 1974, pl. 5, fig. 4).

Hines Ridge, Inyo County, California

UCLA 6156/LACMIP 43374 (Fig. 1.3).—Wyman Formation and Hines member of the Reed Dolomite, S of Waucoba Road and W of Hines Road (37.1020°N, 118.0900°W), sec. 6, T10S, R36E, Waucoba Mountain Quadrangle, California; Ediacaran.

    ?*Gordia* isp. (Fig. 9.1, 9.2; Langille, 1973, 1974; Corsetti and Hagadorn, 2003, fig. 5A).

Mount Dunfee, Esmeralda County, Nevada

JHU 1645, 1648, 1649 (Fig. 1.4; Nelson and Smith, 2019, fig. DR1).—Esmeralda Member, Deep Spring Formation, near Mount Dunfee (37.3429°N, 117.3278°W), Esmeralda County, Nevada; Cambrian (Fortunian).

    Psammichnites gigas arcuatus (Roedel, 1929) (Fig. 12.1, 12.5; Nelson and Smith, 2019, fig. 2A–F, fig. 4A, B; Nelson and Smith, 2020, fig. 1).

Chicago Pass, Inyo County, California

UCLA 7329/LACMIP 43370 (Figs 1.1, 4, Supplemental dataset 1).—Lower member of the Wood Canyon Formation, Chicago Pass (36.1213°N, 116.1788°W) on the Charles Brown Highway (CA route 178), northern end of Nopah Range, Inyo County, California; Ediacaran–Cambrian (Fortunian).

    Didymaulichnus miettensis Young, 1972 (Fig. 11.1).
    Treptichnus pedum (Seilacher, 1955) (Fig. 10.7; Jensen et al., 2002, fig. 4A).
    Treptichnus isp. cf. *T. pedum* (Seilacher, 1955).
    Treptichnus spectrum traces (Fig. 9.7, 9.8).

Spring Mountains, Nye County, Nevada

UCLA 7330/LACMIP 43368 (Figs 1.1, 4, Supplemental dataset 1).—Lower member of Wood Canyon Formation, first wash S of Wood Canyon (36.3852°N, 115.9210°W), Spring Mountains, Nye County, Nevada; Ediacaran–Cambrian (Fortunian).

    Annulated tubular fossils (Fig. 4.5).

Desert Range, Nye County, Nevada

UCLA 7331/LACMIP 43371 (Fig. 1.1, 4, Supplemental dataset 1; Gillett and Van Alstine, 1979).—Lower member, Wood Canyon Formation, ~800 m WSW of National Geodetic Survey benchmark GR0872 (Q 313 1941), Desert National Wildlife Range (36.8039°N, 115.3222°W), Clark County, Nevada, Ediacaran–Cambrian (Fortunian).

    Annulated tubular fossils.
    Treptichnus isp. cf. *T. pedum* (Seilacher, 1955) (Fig. 10.1).

Montgomery Mountains, Nye County, Nevada

UCLA 7333/LACMIP 43369 (Figs. 1.2, 4, Supplemental dataset 1; Horodyski, 1991; Horodyski et al., 1994).—Lower member of the Wood Canyon Formation, 2.8 km WNW of Johnnie (36.419967°N, 116.072604°W), Nye County, Nevada, Ediacaran–Cambrian (Fortunian).

    Tulaneia amabilia Runnegar and Horodyski n. gen. n. sp. (Figs. 5, 6.1–6.7, 7.1–7.9).
    Annulated tubular fossils (Fig. 4.6–4.8).
    Didymaulichnus miettensis Young (1972) (Fig. 11.3; Jensen et al., 2002, fig. 5A).
    Gordia isp. (Fig. 9.4).
    Treptichnus pedum (Seilacher, 1955) (Fig. 10.2, 10.6).
    Treptichnus isp. cf. *T. pedum* (Seilacher, 1955) (Fig. 10.3).
    Treptichnus spectrum traces (Figs. 9.5, 9.6, 10.3, 11.6).

UCLA 7334/LACMIP 43372 (Fig. 1.2, Supplemental dataset 1; Jensen et al., 2002).—Lower member of the Wood Canyon Formation, 3.1 km W of Johnnie (36.419967°N, 116.072604°W), Nye County, Nevada, Ediacaran–Cambrian (Fortunian).

    Rusophycus isp. (Jensen et al., 2002, fig. 4C, 4D).
    Treptichnus pedum (Seilacher, 1955) (Fig. 10.2, 10.6; Jensen et al., 2002, fig. 4B).
    Treptichnus spectrum traces (Fig. 9.6).

NHMLAC 17130/LACMIP 17130 (Fig. 1.1; Hagadorn and Waggoner, 2000; Smith et al., 2017; Selly et al., 2020).—Lower member of the Wood Canyon Formation, SW¼, NW¼, SW¼, sec. 11, T18S, R52E, Mt. Schader Quadrangle, 3.4 km SW of Johnnie, Nye County, Nevada; Ediacaran–Cambrian (Fortunian).

    Saarina hagadorni Selley et al., 2020 (Hagadorn and Waggoner, 2000, fig. 3.7–3.9; Selley et al., 2020, figs. 2B, 2E, 3E)
    ?*Swartpuntia germsi* Narbonne, Saylor, and Grotzinger, 1997 (Hagadorn and Waggoner, 2000, fig. 4.1–4.3).
    ?*Treptichnus pedum* (Seilacher, 1955) (Hagadorn and Waggoner, 2000, fig. 5.8, 5.9).

Ross River, Northern Territory, Australia

UCLA 7346/LACMIP 43373.—Glauconitic sandstones of Member IV of the Arumbera Formation (23.5956°S, 134.4718°E), ~1 km W of the Ross River resort, ~40 km E of Alice Springs, Northern Territory, Australia; Cambrian (Terraneuvian).

    Didymaulichnus miettensis Young, 1972 (Fig. 11.2).
    Psammichnites gigas arcuatus (Roedel, 1929) (Fig. 12.4; McIlroy and Heys, 1997).

Ediacara, South Australia

UNE L1765.—Thinly bedded quartz sandstones near the top of the Ediacara Member, Rawnsley Quartzite on ridge (30.7800°S, 138.1468°E) S of track from Sundown bore to Gap well, Ediacara Hills, W of Beltana, South Australia; Ediacaran.

    Gordia isp. (Fig. 9.3).

Nama Basin, Namibia

UCLA 7322 Swartkloofberg 1 (Runnegar et al., 2024).—Thin sandstones, Nasep Member, Urusis Formation, Schwarzrand Subgroup, Nama Group on dip slope immediately N of Swartkloofberg homestead (27.485491°S, 16.523883°E), Swartkloofberg farm, Rekvlakte 1:50,000 map sheet (2716BC), southern Namibia; Ediacaran.

    Pteridinium carolinaensis (St. Jean, 1973) (Fig. 6.8–6.10).

UCLA 7324 Sonntagsbrunn (Runnegar et al., 2024).—Thin event beds in silt-stones of the Kreyrivier Member, Nomtsas Formation, Schwarzrand Subgroup, Nama Group on E and W sides of hill 850 m on E side of road D463 (27.368114°S, 17.509523°E) ~1.5 km S of Koedoeslaagte homestead, W of the Fish River Canyon, Koedoeslaagte 1:50,000 map sheet (2717DA), southern Namibia; Cambrian (Fortunian).

    Treptichnus pedum (Seilacher, 1955) (Fig. 10.8).